THE EURASIA PROCEEDINGS OF HEALTH, ENVIRONMENT AND LIFE SCIENCES

ISRES Publishing

VOLUME 20 ICMEHES CONFERENCE
ISSN: 2791-8033
ISBN: 978-625-6959-85-9
ICMEHES 2025: 5th International Conference on Medical and Health Sciences (ICMeHeS)
November 12- 15, 2025
Antalya, Türkiye
Edited by: Mehmet Ozaslan (Chair), Gaziantep University, Türkiye

ICMEHES 2025

5th International Conference on Medical and Health Sciences (ICMeHeS)

Proceedings Book

Editor

Mehmet Ozaslan
Gaziantep University, Türkiye

ISBN: 978-625-6959-85-9

Published by the ISRES Publishing

Address: Askan Mah. Akinbey Sok. No: 5-A/Konya/Türkiye

Web: www.isres.org

Contact: isrespublishing@gmail.com

Dates: November 12- 15, 2025

Location: Antalya, Türkiye

https://2025.icmehes.net

About Editor

Prof Dr. Mehmet Ozaslan
Department of Biology, Gaziantep University, Türkiye
Website: mehmetozaslan.com
E-mail: ozaslanmd@gantep.edu.tr

Language Editor

Lecturer Ceren Dogan
School of Foreign Languages, Necmettin Erbakan University, Türkiye
Email: cerendogan@erbakan.edu.tr

CONFERENCE PRESIDENTS

Mehmet Ozaslan - Gaziantep University, Türkiye
Volodymyr Sulyma - Si Dnipropetrovsk Medical Academy, Ukraine

SCIENTIFIC BOARD

Ahmet Ozaslan - Gazi University, Türkiye
Alexander Oleynik - Si Dnipropetrovsk Medical Academy, Ukraine
Aruna M Jarju - King Graduate School-Monroe College, United States
Betül Apaydın Yıldırım - Atatürk University, Türkiye
Cahit Bagci - Sakarya University, Türkiye
David Wortley, International Society of Digital Medicine, United Kingdom
Djamil Krouf - University of Oran, Algeria
Elena Lukianova - Rudn-University, Russia
Eva Trnova - Masaryk University, Czech Republic
Gergely Pápay - Szent István University, Hungary
Gulfaraz Khan - United Arab Emirates University, U.A.E
Harun Ulger - Erciyes University, Türkiye
Ildikó Járdi - Szent István University, Hungary
Iwona Bodys-Cupak, Jagiellonian University Medical College, Poland
Jaleela Alawi - University of Bahrain, Bahrain
Karim Hajhashemi - James Cook University, Australia
Károly Penksza - Szent István University, Hungary
Khandakar A. S. M. Saadat- Gaziantep University, Türkiye
Kristina Kilova - Medical University Plovdiv, Bulgaria
Marinela Asenova Kozhuharova - Shterev Medical Center Reproductive Health, Bulgaria
Mariusz Jaworski - Medical University of Warsaw, Poland
Merita Rumano - University of Tirana, Albania
Mousa Attom- American University of Sharjah, U.A.E
Muhammad Safdar - Cholistan University, Pakistan
Mustafa Saber Al-Attar-Selahaddin University, Iraq
Nigora Muminova - Center for Professional Development of Medical Personal, Uzbekistan
Oltinoy Yakubova - Andijan State Medicine Institute, Uzbekistan
Pınar Gül - Ataturk University, Türkiye
Rıdwan Lawal, Lagos university, Nigeria
Rifat Morina - University of Prizren Ukshin Hoti, Kosovo
Sai Yan - Minzu University of China, China
Teuta Ramadani Rasimi, University of Tetova, Republic of Macedonia
Vladimir Protsenko - Rudn-University, Russia
Volodymyr Sulyma - Si Dnipropetrovsk Medical Academy, Ukraine
Yulduz Rasul-Zade - Tashkent Pediatric Medical Institute, Uzbekistan
Wenxia (Joyl Wu, Eastern Virginia Medical School, U.S.A.
Zhaklina Trajkovska-Anchevska - PHI University Clinic for Hematology-Republic of Macedonia

ORGANIZING COMMITTEE

Aynur Aliyeva - Institute of Dendrology of Anas, Azerbaijan
Dominika Falvai - Szent Istvan University., Hungary
Elman Iskender - Central Botanical Garden of Anas, Azerbaijan
Ishtar Imad - Rasheed University College, Iraq

Editorial Policies

ISRES Publishing follows the steps below in the procedings book publishing process.
In the first stage, the papers sent to the conferences organized by ISRES are subject to editorial oversight. In the second stage, the papers that pass the first step are reviewed by at least two international field experts in the conference committee in terms of suitability for the content and subject area. In the third stage, it is reviewed by at least one member of the organizing committee for the suitability of references. In the fourth step, the language editor reviews the language for clarity.

Review Process

Abstracts and full-text reports uploaded to the conference system undergo a review procedure. Authors will be notified of the application results in three weeks. Submitted abstracts will be evaluated on the basis of abstracts/proposals. The conference system allows you to submit the full text if your abstract is accepted. Please upload the abstract of your article to the conference system and wait for the results of the evaluation. If your abstract is accepted, you can upload your full text. Your full text will then be sent to at least two reviewers for review. **The conference has a double-blind peer-review process.** Any paper submitted for the conference is reviewed by at least two international reviewers with expertise in the relevant subject area. Based on the reviewers' comments, papers are accepted, rejected or accepted with revision. If the comments are not addressed well in the improved paper, then the paper is sent back to the authors to make further revisions. The accepted papers are formatted by the conference for publication in the proceedings.

Aims & Scope

Compared to other fields, developments and innovations in the fields of medical and health sciences are very fast. In this century, where the human population is rapidly increasing and technology is developing rapidly, health problems are constantly changing and new solutions are constantly being brought to these problems. With the Covid 19 epidemic, it has emerged that a health problem affects all humanity and all areas of life. For this reason, this conference focused on the changes and innovations in the field of Medical and Health Sciences.

The aim of the conference is to bring together researchers and administrators from different countries, and to discuss theoretical and practical issues of Medical and Health Sciences. At the same time, it is aimed to enable the conference participants to share the changes and developments in the field of Medical and Health Sciences with their colleagues.

Articles: 1- 6

CONTENTS

The Eurasia Proceedings of Health, Environment and Life Sciences (EPHELS)
ISSN: 2791-8033

The Eurasia Proceedings of Health, Environment and Life Sciences (EPHELS), 2025

Volume 20, Pages 1-6

ICMeHeS 2025: International Conference on Medical and Health Sciences

Immune Alterations in Experimental Type 2 Diabetes Mellitus

Oralbek Ilderbayev
L.N. Gumilyov Eurasian National University

Kerim Mutig
I.M. Sechenov First Moscow State Medical University, RU

Darkhan Uzbekov
L.N. Gumilyov Eurasian National University

Gulzhan Ilderbayeva
L.N. Gumilyov Eurasian National University

Batyrlan Ayash
L.N. Gumilyov Eurasian National University

Zarina Amanova
L.N. Gumilyov Eurasian National University

Abstract: Type 2 diabetes mellitus is a multifactorial metabolic disorder characterized by insulin-independent hyperglycemia, impaired carbohydrate and lipid metabolism, and systemic complications. This study aimed to investigate metabolic and immune alterations in male laboratory rats with experimentally induced T2DM. Forty rats weighing 200 ± 20 g were divided into two groups: control and T2DM. Diabetes was induced via a single intraperitoneal injection of streptozotocin (30 mg/kg), and hyperglycemia was confirmed by fasting blood glucose levels exceeding 7.0 mmol/L. Metabolic analysis revealed significant hyperglycemia (20% increase, $p<0.05$), elevated immunoreactive insulin and C-peptide concentrations ($p<0.05$), and a trend toward increased glycated hemoglobin (HbA1c), indicating compensatory β-cell hyperactivity and early-stage metabolic dysregulation. Immunological assessment showed decreased total leukocyte and lymphocyte counts, with pronounced reductions in T-lymphocytes (CD3+) and T-helper cells (CD4+) ($p<0.05$), while T-suppressor cells (CD8+) remained unchanged, resulting in a reduced CD4/CD8 ratio. Functional tests demonstrated impaired lymphocyte mitogenic response, reduced antibody-forming cell activity, and suppressed natural killer cell activity ($p<0.01$), suggesting compromised innate and adaptive immunity. These findings indicate that experimental T2DM induces a combination of metabolic disturbances and systemic immune dysfunction. The observed interplay between hyperglycemia, β-cell stress, and immune suppression may contribute to increased susceptibility to infections and chronic inflammatory processes. Understanding these early alterations provides insight into the pathogenesis of T2DM and may inform the development of therapeutic strategies targeting both metabolic and immune pathways.

Keywords: Type 2 diabetes mellitus, Streptozotocin, Immunity

Introduction

Currently, the complex impact of chronic metabolic conditions, such as diabetes mellitus, on the human body is attracting significant attention from the scientific community. Type 2 diabetes mellitus (T2DM) is a

multifactorial disease characterized by insulin-independent hyperglycemia and disturbances in carbohydrate and lipid metabolism, developing at the intersection of metabolic, hormonal, and immunological dysfunctions. Two main clinical types of diabetes are distinguished: type 1 diabetes mellitus (T1DM) and type 2 diabetes mellitus (T2DM). T1DM is characterized by the autoimmune destruction of pancreatic β-cells, resulting in a complete cessation of insulin production. T2DM is more prevalent in adults and is associated with obesity, reduced physical activity, and genetic predisposition. In this form, insulin may be produced in sufficient quantities, but target cells exhibit decreased sensitivity, leading to the development of insulin resistance (Dedov et al., 2023, American Diabetes Association, 2024).

If diabetes remains uncontrolled over time, various systemic complications may develop, including angiopathies, nephropathy, retinopathy, and cardiovascular diseases, such as myocardial infarction and stroke (Tomic et al., 2022). Recent studies also indicate that immune system function is altered even in T2DM, playing a significant role in the pathogenesis of these complications. While disruptions in carbohydrate metabolism and insulin deficiency affect immune responses, the immune system itself actively contributes to the progression of diabetes.

T1DM is an autoimmune disease in which the body's immune system recognizes insulin-producing β-cells of the pancreas as foreign and destroys them. T-lymphocytes play a key role in this autoimmune reaction, recognizing antigens on the β-cell surface and initiating cytotoxic responses (Chen et al., 2024; Esser et al., 2014). In T2DM, hyperglycemia and insulin resistance exert systemic effects on the immune system by reducing lymphocyte functional activity and altering cytokine balance, thereby weakening the body's defense against infectious agents.

As a result, individuals with diabetes show increased frequency and severity of infections affecting the skin, genitourinary system, and respiratory tract. Additionally, T-cell dysfunction is commonly observed in diabetic patients, further contributing to impaired immune responses and the development of chronic subclinical inflammation (Todd,2010; Tkachuk et al., 2014). Chronic hyperglycemia also induces oxidative stress and elevates lipid peroxidation, adversely affecting immune cell membrane structure and energy metabolism, which reduces the effectiveness of immune responses.

Thus, diabetes mellitus is not only a metabolic disorder but also a pathology that exerts complex effects on the immune system. This dual impact contributes to the increased incidence of infectious and inflammatory complications in patients, as well as reduced efficacy of therapeutic interventions, highlighting the importance of considering immune parameters in clinical management.

Study Objectives

The study of immunological parameters in experimental modeling of type 2 diabetes mellitus in animals.

Methods

To achieve the stated objective, an experiment consisting of four series was conducted on 40 male white laboratory rats weighing 200 ± 20 g, maintained under vivarium conditions. Group I served as the control, while Group II included animals in which type 2 diabetes mellitus (T2DM) was experimentally induced. The rats were euthanized under ether anesthesia using a partial decapitation method, in accordance with the requirements of the local ethics committee and the international principles of humane treatment of animals outlined in the Helsinki Declaration (World Medical Association, 2002).

Type 2 diabetes mellitus was induced using streptozotocin (MP Biomedicals, USA), a compound that selectively targets pancreatic β-endocrinocytes. The drug was administered intraperitoneally at a dose of 30 mg/kg. This model is considered the closest pathogenetically relevant representation of human type 2 diabetes. To confirm the development of T2DM, fasting blood glucose levels were measured two weeks after streptozotocin administration. The inclusion criterion for the T2DM group was a glucose concentration exceeding 7.0 mmol/L.

Assessment of Metabolic Parameters. Blood glucose levels were determined using an express method with a glucometer. Glycated hemoglobin (HbA1c) was measured as an indicator of persistent hyperglycemia. The

functional activity of pancreatic β-cells and the degree of insulin resistance were assessed by measuring C-peptide levels in serum and immunoreactive insulin concentrations in plasma using specific assay kits.

Assessment of Immunological Parameters. Total leukocyte and lymphocyte counts in peripheral blood were determined for all experimental animals. The numbers of B- and T-lymphocytes and their subpopulations were assessed using immunofluorescent staining with FITC-conjugated antibodies. Stained cells were examined under a fluorescence microscope. For quantitative analysis, the immunoregulatory index (IRI) was calculated. The leukocyte migration inhibition reaction (LMIR) was performed using phytohemagglutinin (PHA) (Clausen, 1975). The concentration of circulating immune complexes (CIC) was determined (Jin et al., 2024), and neutrophil activity was assessed using the nitroblue tetrazolium (NBT) test (Damle et al., 2022).

Statistical Analysis. Statistical analysis was performed using STATISTICA 8.0 software. Group data were presented as mean ± standard deviation (M ± SD). The significance of differences between groups was evaluated using Student's t-test.

Results and Discussion

Metabolic Alterations. In the diabetic group of rats, a significant 20% increase in blood glucose levels was observed ($p<0.05$), reflecting the development of persistent hyperglycemia characteristic of this pathology. Simultaneously, the concentrations of immunoreactive insulin and C-peptide were elevated ($p<0.05$), which may indicate compensatory hypersecretion of insulin by pancreatic β-cells in response to developing insulin resistance. The level of glycated hemoglobin showed a tendency to increase, confirming the chronic nature of carbohydrate metabolism disturbances. Together, these changes correspond to the metabolic profile of the early stages of type 2 diabetes mellitus, when hyperglycemia is accompanied by compensatory stress on the insulin system (Table1).

Table 1. Changes in metabolic parameters of the experimental animals

Indications	I- control group	II – Experimental group
Glucose concentration, mmol /L	6,02±0,32	7,25±0,52*
Glycated hemoglobin, %	2,85±0,22	3,35±0,23
Immunoreactive insulin, ng /mL	0,64±0,09	0,87±0,07*
C-peptide, ng /mL	2,01±0,2	2,95±0,19*

Note: The difference is significant compared to the control group * - $p<0,05$; ** - $p<0,01$.

The elevation of glucose and glycated hemoglobin not only reflects impaired glucose utilization by tissues but also the activation of non-enzymatic protein glycation processes, leading to the formation of advanced glycation end-products (AGEs). These compounds can cause vascular damage, enhance oxidative stress, and activate inflammatory signaling pathways. Even moderate hyperglycemia can initiate a cascade of secondary pathological reactions, subsequently exacerbating endothelial dysfunction and metabolic instability.

The increased concentrations of immunoreactive insulin and C-peptide in diabetic animals are likely associated with compensatory hyperfunction of pancreatic β-cells. At the early stages of type 2 diabetes, β-cells attempt to overcome reduced insulin sensitivity of peripheral tissues by increasing insulin secretion; however, prolonged secretory stress ultimately depletes the insulin pool and reduces the functional reserve of the pancreas. Elevated C-peptide levels confirm preserved proinsulin secretion and reflect an adaptive response to rising insulin resistance.

Thus, the metabolic alterations observed in animals with experimental type 2 diabetes are characterized by chronic hyperglycemia, hyperinsulinemia, and activation of protein glycation processes, collectively creating a predisposition to systemic metabolic and inflammatory disturbances. These findings are consistent with literature reports indicating that prolonged carbohydrate metabolism impairment in diabetic animals leads to a complex of biochemical and endocrine adaptations aimed at maintaining energy homeostasis but with pathological consequences at tissue and organ levels.

Immune System Changes. Immunological parameters demonstrated pronounced shifts in the cellular component of the immune system. In diabetic animals, total leukocyte and lymphocyte counts were decreased ($p<0.05$), indicating reduced overall immune reactivity. Notably, T-lymphocytes (CD3+) and T-helper cells (CD4+) were significantly reduced in both absolute and relative terms ($p<0.05$), reflecting suppression of the T-cell compartment and disruption of cooperation among immune-competent cells. Meanwhile, T-suppressor cell

(CD8+) levels remained largely unchanged, leading to a reduction in the immunoregulatory index (CD4/CD8) and a shift of immune balance toward suppressor influence (Table 2).

Table 2. Changes in immune system parameters of the experimental animals

Indications		I- control group	II – Experimental group
WBC, $\times 10^9$/l	Abs. number	6,26±0,36	5,20±0,37 *
Lymphocytes, $\times 10^9$/l	Abs. number	2,61±0,16	2,18±0,14 *
	%	35,78±2,17	33,64±2,05
T-lymphocytes (CD3+), $\times 10^9$/l	Abs. number	1,58±0,09	1,30±0,10 *
	%	29,55±1,47	24,63±1,83 *
T-helpers (CD4+), $\times 10^9$/l	Abs. number	0,75±0,05	0,61±0,04 *
	%	18,48±1,54	14,58±1,13*
T-suppressors (CD8+), $\times 10^9$/l	Abs. number	0,56±0,03	0,50±0,03
	%	11,43±0,63	10,11±0,64
B-lymphocytes (CD20+) $\times 10^9$/l	Abs. number	0,43±0,03	0,48±0,03
	%	6,64±0,48	7,76±0,53
IRI (CD4/CD8)	-	1,34±0,07	1,22±0,08
LMIR	index	0,88±0,05	1,04±0,06 *
Circulating immune complexes (CIC)	conditional unit	1,36±0,08	1,12±0,08 *
Nitro blue tetrazolium (NBT-test)	%	3,78±0,26	2,44±0,18 **

Note: The difference is significant compared to the control group * - $p<0,05$; ** - $p<0,01$.

Increases in the lymphocyte mitogenic response index (LMTR) and decreases in antibody-forming cell (AFC) responses, as well as a significant reduction in natural killer (NK) cell activity ($p<0.01$), indicate impaired phagocytic and cytotoxic functions of innate immune cells. These changes are likely associated with oxidative stress, hyperglycemia, and disrupted lymphocyte metabolism in chronic diabetes. The reduction in CD3+ and CD4+ cells aligns with literature describing immunodeficiency in prolonged type 2 diabetes, which is linked to thymic dysfunction and T-cell apoptosis.

Chronic hyperglycemia leads to the accumulation of glycated proteins and lipid peroxides, acting as autoantigens and causing dysfunction of T- and B-lymphocytes. In type 2 diabetes, the production of pro-inflammatory cytokines (IL-1β, IL-6, TNF-α) is activated, promoting chronic subclinical inflammation and secondary exhaustion of immune responses. The decrease in T-helper cells with preserved B-lymphocytes (CD19+) indicates disrupted coordination between cellular and humoral immunity, reducing lymphocyte responsiveness to antigenic stimulation and potentially increasing susceptibility to infections.

Weakened NK-cell activity and reduced phagocytic capacity further indicate impaired innate immune defense. These alterations are likely related to membrane damage and impaired energy metabolism of immune cells under chronic oxidative stress. Hyperglycemia and elevated reactive oxygen species reduce the expression of pattern recognition receptors (PRRs) on monocytes and macrophages, impairing their phagocytic and antigen-presenting capabilities.

The results confirm the presence of systemic immune dysfunction in experimental type 2 diabetes. Metabolic disturbances, including hyperglycemia and hyperinsulinemia, are closely associated with immunodeficiency, forming a vicious cycle that exacerbates pathogenic processes. The observed combination of chronic metabolic stress and impaired immune competence may contribute to the development of diabetic complications, including increased susceptibility to infections, delayed wound healing, and chronic inflammatory foci. These findings highlight the interplay between metabolic and immune dysregulation, emphasizing the importance of targeting both pathways for therapeutic interventions.

Conclusion

Based on the data obtained, the following conclusions can be drawn regarding the complex alterations in animals with experimental type 2 diabetes mellitus. Experimental hyperglycemia was accompanied by a significant increase in blood glucose, immunoreactive insulin, and C-peptide levels, reflecting a state of compensated insulin resistance and β-cell activation in the pancreas. Concurrently, there was a trend toward increased glycated hemoglobin, indicating the chronic nature of carbohydrate metabolism disturbances and the

activation of non-enzymatic protein glycation processes, which contribute to oxidative stress and subclinical inflammation.

Metabolic disturbances were directly associated with immunodeficient changes. A decrease in the number of leukocytes, lymphocytes, T-lymphocytes (CD3+), and T-helper cells (CD4+) combined with a preserved level of T-suppressors (CD8+) resulted in immune imbalance and reduced immunoregulatory index (CD4/CD8). At the same time, reduced natural killer cell activity and phagocytic capacity indicate impaired innate immunity. These alterations can be explained by the effects of hyperglycemia and glycated products on immune cell membranes, as well as the activation of pro-inflammatory cytokines, which create a state of chronic low-grade inflammation.

Thus, experimental type 2 diabetes mellitus in rats is accompanied by the formation of a complex metabolic and immune homeostasis imbalance. Metabolic disturbances promote the development of immunodeficiency, while impaired immune defense further exacerbates the pathogenic processes of diabetes. These findings highlight the interrelationship between hyperglycemia, insulin resistance, and cellular immune dysfunction, which is crucial for understanding the mechanisms of diabetic complications and developing therapeutic strategies aimed at correcting both metabolic and immune disturbances.

Scientific Ethics Declaration

* The authors declare that the scientific ethical and legal responsibility of this article published in EPHELS journal belongs to the authors.

Conflicts of Interest

* The authors declare no conflict of interest.

Funding

* This research was funded by the Science Committee of the Ministry of Science and Higher Education of the Republic of Kazakhstan, Grant No. AP26198141.

Acknowledgements or Notes

* This article was presented as a poster presentation at the International Conference on Medical and Health Sciences (www.icmehes.net) held in Antalya/Türkiye on November, 12-15, 2025.

References

American Diabetes Association Professional Practice Committee. (2024). Introduction and methodology: Standards of care in diabetes. *Diabetes Care, 47*(1), 1–4.

Chen, Y., Huang, R., Mai, Z., Chen, H., Zhang, J., Zhao, L., Yang, Z., Yu, H., Kong, D., & Ding, Y. (2024). Association between systemic immune-inflammatory index and diabetes mellitus: Mediation analysis involving obesity indicators in the NHANES. *Frontiers in Public Health, 11*, 1331159.

Clausen, J. E. (1975). Migration inhibition of human leukocytes mixed with phytohemagglutinin-preincubated mononuclear leukocytes. *Acta Allergologica, 30*(5), 239–249.

Damle, V. G., Wu, K., Arouri, D. J., & Schirhagl, R. (2022). Detecting free radicals post viral infections. *Free Radical Biology and Medicine, 191*, 8–23.

Dedov, I. I., & Shestakova, M. V. (2023). *Diabetes mellitus: A guide for physicians* (p.456). GEOTAR-Media.

Esser, N., Legrand-Poels, S., Piette, J., Scheen, A. J., & Paquot, N. (2014). Inflammation as a link between obesity, metabolic syndrome and type 2 diabetes. *Diabetes Research and Clinical Practice, 105*, 141–150.

Jin, X., Li, D., …& Quan, W. (2024). Leaky gut, circulating immune complexes, arthralgia, and arthritis in IBD: Coincidence or inevitability? *Frontiers in Immunology, 15*,1347901.

Todd, J. A. (2010). Etiology of type 1 diabetes. *Immunity, 32*(4), 457–467.

Tkachuk, V. A., & Vorotnikov, A. V. (2014). Molecular mechanisms of development of insulin resistance. *Diabetes Mellitus, (2),* 29–40.

Tomic, D., Shaw, J. E., & Magliano, D. J. (2022). The burden and risks of emerging complications of diabetes mellitus. *Nature Reviews Endocrinology, 18*, 525–539.

World Medical Association. (2002). *Declaration of Helsinki: Ethical principles for medical research involving human subjects* (pp.42–46). UMS.

Author(s) Information

Oralbek Ilderbayev
L.N. Gumilyov Eurasian National University
010008 Astana, Satpayev 2, Kazakhstan.
Contact e-mail: *oiz5@yandex.ru*

Kerim Mutig
I.M. Sechenov First Moscow State Medical University, Russia

Darkhan Uzbekov
L.N. Gumilyov Eurasian National University
010008, Kazakhstan, Astana, Satpayev 2 Kazakhstan

Gulzhan Ilderbayeva
L.N. Gumilyov Eurasian National University
010008, Kazakhstan, Astana, Satpayev 2, Kazakhstan

Batyrlan Ayash
L.N. Gumilyov Eurasian National University
010008, Astana, Satpayev 2 Kazakhstan

Zarina Amanova
L.N. Gumilyov Eurasian National University
010008, Astana, Satpayev 2 Kazakhstan

To cite this article:

Ilderbayev, O., Mutig, K., Uzbekov, D., Ilderbayeva G., Ayash B., & Amanova Z. (2025). Immune alterations in experimental type 2 diabetes mellitus. *The Eurasia Proceedings of Health, Environment and Life Sciences (EPHELS), 20,* 1-6.

The Eurasia Proceedings of Health, Environment and Life Sciences (EPHELS)
ISSN: 2791-8033

The Eurasia Proceedings of Health, Environment and Life Sciences (EPHELS), 2025

Volume 20, Pages 7-13

ICMeHeS 2025: International Conference on Medical and Health Sciences

The Ecological, Chemical, Biological and Medical Condition of the Aral Sea Region

Lobar Sharipova
Kazan Federal University (Jizzakh Branch)

Anastasiya Shakirova
Kazan Federal University (Jizzakh Branch)

Sabina Yusufova
Kazan Federal University (Jizzakh Branch)

Dilfuza Kholbaeva
Kazan Federal University (Jizzakh Branch)

Gavkhar Turaeva
Kazan Federal University (Jizzakh Branch)

Iroda Alikulova
Kazan Federal University (Jizzakh Branch)

Nazira Khaydarova
Kazan Federal University (Jizzakh Branch)

Ikrom Ruzmatov
Kazan Federal University (Jizzakh Branch)

Abstract: This article thoroughly examines the ecological state of the Aral Sea region and its impact on human health, particularly from medical, biological, chemical, and microbiological perspectives. The ecological crisis caused by the drying of the Aral Sea poses a serious threat not only to the environment but also to public health. As the water level has decreased and the seabed has dried up, large amounts of salt and dust have been released into the air, increasing the concentration of heavy metals, pesticides, and other toxic substances in the atmosphere. This has led to a rise in respiratory, cardiovascular, oncological, and allergic diseases. Additionally, internal diseases such as liver, kidney, and gastrointestinal disorders are frequently observed, largely due to the poor quality of drinking water and food products. Dental diseases, including caries, periodontitis, and gum inflammations, are also widespread in the region, which is linked to the deterioration in water quality, deficiency of essential microelements, and chemically-influenced oral hygiene conditions. Pollution of soil and water resources disrupts the biological balance, negatively affecting plant and animal life. Changes in the microbiological environment have also increased the risk of infectious diseases. The article provides a scientific analysis of the medical and biological consequences of environmental degradation and offers recommendations aimed at protecting public health and restoring ecological stability.

Keywords: Aral Sea region ecosystem, Biological diversity, Dust particles, Human health, Chemical pollution

Introduction

Until the mid-20th century, the Aral Sea was a vast body of water teeming with life. Covering an area of about 68,000 square kilometers, it was a unique ecosystem rich in biodiversity that helped create a moderate climate amid the vast deserts and steppes of Central Asia. The sea received water from two major rivers - the Amu Darya and the Syr Darya (Khurramov, 2025).

For the people living in the regions surrounding the Aral Sea, the sea was the main source of livelihood. The fishing industry thrived - tens of thousands of tons of fish were caught annually, and canning factories operated actively. Life was bustling in port cities such as Muynak and Aral. The sea also served as an important transportation route, used for carrying both cargo and passengers. The Aral's mild climate created favorable conditions for agriculture and livestock farming in the surrounding areas. The sea was a source of life and prosperity for the people of the region (Sharipova et al., 2024).

Method

Roots of the Tragedy

The main cause of the Aral Sea disaster lies in the massive irrigation projects launched in the 1960s to expand large-scale irrigated agriculture. Huge amounts of water from the Amu Darya and Syr Darya rivers were diverted through canals to irrigate cotton and other crop fields (Sharipova, 2022). Since most of the canals in these projects were dug directly into the soil without proper lining, a significant portion of the water - according to some estimates, between 30% and 70% - was lost through seepage and evaporation. As a result, the amount of river water flowing into the Aral Sea decreased sharply. While before 1960 the sea received an average of 50–60 cubic kilometers of water annually, by the 1980s this figure had dropped to almost zero. The halt in water inflow caused the sea level to fall rapidly, leading to its desiccation (Alikhanova et al., 2023). The drying up of the Aral Sea brought about unprecedented negative consequences for the region and the entire world.

Results and Discussion

Environmental Consequences

Disappearance of the Sea

The surface area of the Aral Sea shrank several times over, and its water level dropped by more than 20 meters. Salinity increased sharply - in some areas, several times higher than that of ocean water. The sea split into two parts (the North Aral and the South Aral), and later into three separate water bodies (Shamshetdinova, 2025). In the place of the dried-up sea, a new desert called the Aralkum emerged, covering more than 5.5 million hectares. This desert is coated with toxic salts, pesticides, and residues of chemical fertilizers (Chida, 2020).

Climate Change

The Aral Sea ceased to serve as a natural air conditioner that moderated the regional climate. As a result, the climate became sharply continental: summers grew hotter and drier, while winters became colder and longer. The growing season shortened, and precipitation levels decreased (Ignatieva, et al., 2023).

Dust and Salt Storms

Every year, millions of tons of toxic dust and salt rise from the Aralkum Desert and are carried by winds over thousands of kilometers. These pollutants spread not only across Central Asia but also reach Eastern Europe, Scandinavia, and even the Arctic glaciers. They cause severe damage to human health, agriculture, and ecosystems (Bazarbayev, et al., 2022).

Loss of Biodiversity

As the salinity of the sea increased, nearly all fish species - once numbering over 30 - became extinct. Aquatic and coastal ecosystems, including unique tugai (riparian) forests, degraded severely. Many animal and bird species disappeared or were forced to migrate to other habitats (Ivanova, 2023).

The ecological impact of the Aral Sea's desiccation affected not only human health but also the surrounding environment — particularly soil composition and the life of microorganisms within it. The reduction in soil moisture eliminated the conditions necessary for microbial life. Some beneficial bacteria, such as nitrogen-fixing and organic matter-decomposing species, perished because they could not withstand the drought (Anchitate al., 2021).

As a result, biological activity declined, and the soil's natural ability to regenerate was lost. Many beneficial bacteria and fungi perished. Microbiological diversity decreased, and the number of useful microorganisms dwindled. In the saline environment, only certain halophilic (salt-tolerant) microorganisms survive. The population of bacteria that decompose organic matter declined, slowing the formation of humus. Nitrogen cycling in the soil was disrupted, and the uptake of elements such as phosphorus and potassium deteriorated (Kirillin et al., 2025). Beneficial bacteria, such as rhizobia bacteria, live in symbiosis with plant roots. In a saline environment, plants cannot effectively absorb nutrients. As a result, crop yields decrease.

Socio-Economic Consequences

Collapse of the Fishing Industry

The fishing industry, which employed thousands of people, along with related enterprises such as canning factories and ship repair workshops, completely collapsed. This led to economic decline in cities like Muynak and many surrounding villages (Uysal et al., 2026).

Unemployment and Migration

The loss of jobs led to widespread unemployment and forced people to move to other regions (environmental migration). Many once-thriving settlements were abandoned.

Damage to Agriculture

Salty dust settled on crop fields, reducing soil fertility and lowering yields. Water shortages and secondary soil salinization created serious problems for farming. Livestock farming also suffered as the quality of pastures declined (Kumar, 2023).

Health Problems

Due to dust and salt storms, the deterioration of drinking water quality, and the overall harsh environmental conditions, the incidence of various diseases has increased, including:

Respiratory Diseases

Among the population of the Aral region, respiratory illnesses such as asthma, bronchitis, tuberculosis, and allergic conditions have become widespread.

Maternal and Child Health

Children frequently suffer from congenital defects, developmental disorders, rickets, and low birth weight.

Dental and Oral Health Issues

The effects of acidic and salty water, along with mineral and vitamin deficiencies in food, have led to numerous dental problems, including caries, fluorosis, gingivitis and periodontitis, tooth erosion and demineralization, and stomatitis.

Cardiovascular Diseases

Hypertension, ischemic heart disease, stroke risk, and atherosclerosis have become more prevalent.

Diseases of the Liver, Kidneys, and Abdominal Organs

Hepatitis (especially types A and E), liver inflammation, cirrhosis, kidney stones, pyelonephritis, and gastrointestinal disorders such as gastritis, ulcers, and dysentery.

Oncological (Cancer) Diseases

Lung, liver, skin, and colorectal cancers, as well as leukemia in children.

Skeletal and Bone System Disorders

Caused by excessive fluoride and other substances in the water. These include osteoporosis, arthritis, arthrosis, and improper bone development in children.

Ways to Mitigate the Problem and Solutions

Completely solving the Aral Sea problem - that is, restoring the sea to its former state — is currently considered nearly impossible (see Figure 1). However, comprehensive measures are necessary to mitigate its negative consequences, improve the living conditions of the regional population, and stabilize the ecosystem (Sharipova et al., 2019).

Figure 1. The current state of the Aral Sea

Today, the fate of the Aral Sea is divided into two parts. With the efforts of the Kazakh government and international organizations, the Kokaral Dam was constructed on the Syr Darya channel. This enabled the water level of the North Aral Sea (Small Aral) to rise somewhat, reduced salinity, and allowed partial restoration of the fishing industry. Although this successful project has offered a glimmer of hope, a full return of the sea to its original state remains extremely difficult (Sharipova, 2022). The South Aral Sea (Large Aral), however, has almost completely dried up, and its future remains highly uncertain. It is now divided into two extremely saline, shallow water basins - western and eastern. The eastern part remains entirely dry for most of the year. The inflow of water from the Amu Darya River to the sea is still very limited (Sharipova et al., 2023).

The government of Uzbekistan is working to reduce the amount of toxic dust and salt rising from the Aralkum Desert by creating large-scale forests on the dried seabed and planting Saxaul and other desert plants (Yusufova, 2023). Significant efforts are being made to establish these "Green Covers." Considering soil conditions, sand, and salinity, only carefully selected seedlings can survive. To maintain greenery in the western basins of the Aral region, it is necessary to study the suitability of desert plants to the dried seabed. For this purpose, seeds and seedlings of desert plants such as Kasson saxaul, Kandym, and Koraburoq are being planted because of their adaptability to the environment (Yusufova, 2023).

Efficient Water Resource Management

Strengthen cooperation among Central Asian countries for the fair and rational distribution of water resources. Widely implement water-saving technologies in agriculture, such as drip and sprinkler irrigation (Yusufova, 2023). Modernize canals and irrigation systems to reduce water losses. Shift to cultivating crops that require less water and are salt-tolerant, and diversify agricultural production.

Environmental Measures

Continue and expand afforestation programs on the dried seabed of the Aral Sea (Saxaul planting). Preserve and restore local ecosystems, including tugai forests and lakes. Support projects aimed at protecting biodiversity. Monitor dust and salt storms and implement measures to reduce their impact (Yusufova, 2023).

Socio-Economic Development

Create new jobs for the population of the Aral region and develop alternative sources of income, such as ecotourism and adapted forms of livestock farming. Improve the healthcare system and provide the population with access to clean drinking water. Support education and vocational training programs. Develop infrastructure, including roads and communication networks (Shakirova, 2023).

International Cooperation

Strengthen the activities of the International Fund for Saving the Aral Sea (IFAS). Develop cooperation with the UN, World Bank, Asian Development Bank and other international organizations and donor countries, attracting financial and technical assistance.

Support Scientific Research on the Aral Sea Problem and Facilitate the Exchange of Knowledge and Experience

There are still many challenges in mitigating the Aral Sea problem. These include regional disputes over water distribution, the negative impact of climate change on water resources (such as glacier melting), insufficient funding for project implementation, and the severity of socio-economic problems in certain areas (Shakirova et al., 2025).

The future largely depends on the unity and political will of Central Asian countries, as well as the support of the international community. While full restoration of the Aral Sea is impossible, the experience of the North Aral demonstrates that targeted efforts can bring positive changes. From now on, the main focus should shift from restoring the sea to adapting to the current situation, minimizing the consequences of the ecological disaster, ensuring sustainable development in the Aral region, and improving the lives of its people.

Conclusion

The Aral Sea disaster serves as a bitter lesson on how disastrous the consequences of humanity's thoughtless actions toward nature can be. This problem is not only ecological but also has profound social, economic, and humanitarian dimensions. Although restoring the sea to its former state may seem impossible, much remains to be done to mitigate its negative impacts, stabilize life in the region, and create a sustainable environment for

future generations. Achieving this requires strengthening regional cooperation, rational use of water resources, implementing modern technologies, and ensuring continuous support from the international community.

Scientific Ethics Declaration

* The authors declare that the scientific ethical and legal responsibility of this article published in EPHELS journal belongs to the authors.

Conflicts of Interest

* The authors declare no conflict of interest.

Funding

* This research received no specific grant from any funding agency in the public, commercial, or not-for-profit sectors.

Acknowledgements or Notes

* This article was presented as a poster presentation at the International Conference on Medical and Health Sciences (www.icmehes.net) held in Antalya/Türkiye on November 12-15, 2025.

References

Alikhanova, S., & Bull, J. W. (2023). Review of nature-based solutions in dryland ecosystems: The Aral Sea case study. *Environmental Management, 72*, 457–472.

Anchita, Z., Zhupankhan, A., Khaibullina, Z., Kabiyev, Y., Persson, K. M., & Tussupova, K. (2021). Health impact of drying Aral Sea: One Health and socio-economical approach. *Water, 13*(22),Article 3196.

Bazarbayev, R., Zhou, B., Allaniyazov, A., et al. (2022). Physical and chemical properties of dust in the Pre-Aral region of Uzbekistan. *Environmental Science and Pollution Research, 29*, 40 893–40 902.

Chida, T. (2020). The Perestroika and environmental issues: The politics of the 'Aral Sea problems'. *International Relations, 201*, 201.

Ignatieva, N. O., & Runkov, S. I. (2023). Environmental and socio-economic problems of the Aral Sea. *Ogarëv-online, 11*(4), 1-6.

Ivanova, M. (2023). Study on the Aral Sea crisis from the risk assessment of polycyclic aromatic hydrocarbons and organochlorine pesticides in surface water of Amu Darya River Basin in Uzbekistan. *Frontiers in Earth Science, 11*, 1295485.

Khurramov, S. (2025). The Aral Sea tragedy: History, consequences, and future. *Journal of Society*, *3*,192

Kirillin, G., Shatwell, T., & Izhitskiy, A. S. (2025). Consequences of the Aral Sea restoration for its present physical state: Temperature, mixing, and oxygen regime. *Hydrology and Earth System Sciences, 29*, 3569.

Kumar, S. (2023). The Aral Sea, situated among five Central Asian republics, has dramatically shrunk …. *International Journal of Geography, Geology and Environment, 5*(1), 211–226.

Shakirova, A. P. (2023). Features of teaching medical parasitology to first-year students at the medical faculty. *International Scientific Journal: News of Education – Research in the 21st Century, 10*(100, Part 2), 277.

Shakirova, A. P., & Tursunbaeva, S. F. (2025). The use of artificial intelligence in teaching biology at school. In *Modern Problems of Intelligent Systems: Republican Scientific and Practical Conference* (p. 70). Jizzakh.

Shamshetdinova, Y. P. (2025). The influence of environmental factors of the Aral Sea region on the development of dentoalveolar anomalies in children. *International Journal of Medical Sciences*, 16–23.

Sharipova, L. A. (2022). Ecological efficiently of mechanochemical synthesis. *Science and Innovation*, 7188379

Sharipova, L. A. (2022). *Synthesis, structure and properties of coordination compounds of zinc nitrate with homogeneous and mixed ligand ligands* (Doctoral dissertation). Bukhara State University.

Sharipova, L. A., Azizov, T. A., Ibragimova, M. R., & Kholmatov, D. S. (2019). New coordination compounds of zinc nitrate with nitrocarbamide, benzamide and benzoic acid. *NamSU Scientific Bulletin, 1*(3), 42–48.

Sharipova, L. A., Azizov, T. A., Ibragimova, M. R., & Mamatova, F. K. (2023). Complex compound of zinc nitrate based on formamide and nicotinic acid. *Universum: Chemistry and Biology, 4*(106), 65–68.

Sharipova, L. A., Ibragimova, M. R., Khudoyberganov, O. I., Khallokov, F. K., Bobakulov, Kh. M., & Abdullaeva, Z. Sh. (2024). Synthesis and study of the complex compound of isonicotinamide with zinc nitrate. *The Eurasia Proceedings of Science, Technology, Engineering & Mathematics (EPSTEM), 30*, 47–55.

Uysal Oğuz, C., Özkan, A., & Özer, S. (2026). Socio-economic and environmental dimensions of the Aral Sea disaster from the sustainable development perspective. *Bilig*, 7670.

Yusufova, S. G. (2023). Basics of titrimetric methods of analysis. *Spectrum Journal of Innovation, Reforms and Development, 20*, 61–63.

Yusufova, S. G. (2023). Development of ideas about colloidal disperse systems and their basic properties. *Western European Journal of Modern Experiments and Scientific Methods, 1*(3), 73–77.

Yusufova, S. G. (2023). Redox processes. *American Journal of Interdisciplinary Research and Development, 21*, 132–135.

Yusufova, S. G. (2023). The subject and ways of development of organic chemistry: The main stages in the development of organic chemistry. *Eurasian Journal of Learning and Academic Teaching, 21*, 87–91.

Author(s) Information

Lobar Sharipova
Kazan Federal University (Jizzakh Branch)
Branch of Kazan (Volga Region) Federal University in the city of Jizzakh, 130000, Jizzakh city, Jizzakhlik mahalla, Sharof Rashidov street, 295. Republic of Uzbekistan,
Contact e-mail: *sharipovalobar82@gmail.com*

Anastasiya Shakirova
Kazan Federal University (Jizzakh Branch)
Branch of Kazan (Volga Region) Federal University in the city of Jizzakh, 130000, Jizzakh city, Jizzakhlik mahalla, Sharof Rashidov street, 295, Republic of Uzbekistan

Sabina Yusufova
Kazan Federal University (Jizzakh Branch)
Branch of Kazan (Volga Region) Federal University in the city of Jizzakh, 130000, Jizzakh city, Jizzakhlik mahalla, Sharof Rashidov street, 295, Republic of Uzbekistan

Dilfuza Kholbaeva
Kazan Federal University (Jizzakh Branch)
Branch of Kazan (Volga Region) Federal University in the city of Jizzakh, 130000, Jizzakh city, Jizzakhlik mahalla, Sharof Rashidov street, 295, Republic of Uzbekistan

Gavkhar Turaeva
Kazan Federal University (Jizzakh Branch)
Branch of Kazan (Volga Region) Federal University in the city of Jizzakh, 130000, Jizzakh city, Jizzakhlik mahalla, Sharof Rashidov street, 295, Republic of Uzbekistan

Iroda Alikulova
Kazan Federal University (Jizzakh Branch)
Branch of Kazan (Volga Region) Federal University in the city of Jizzakh, 130000, Jizzakh city, Jizzakhlik mahalla, Sharof Rashidov street, 295, Republic of Uzbekistan

Nazira Khaydarova
Kazan Federal University (Jizzakh Branch)
Branch of Kazan (Volga Region) Federal University in the city of Jizzakh, 130000, Jizzakh city, Jizzakhlik mahalla, Sharof Rashidov street, 295, Republic of Uzbekistan

Ikrom Ruzmatov
Kazan Federal University (Jizzakh Branch)
Branch of Kazan (Volga Region) Federal University in the city of Jizzakh, 130000, Jizzakh city, Jizzakhlik mahalla, Sharof Rashidov street, 295, Republic of Uzbekistan

To cite this article:

Sharipova, L, Shakirova, A., Yusufova, S., Kholbaeva, D., Turaeva, G., Alikulova, I., Khaydarova, N. & Ruzmatov, I. (2025). The ecological, chemical, biological and medical conditions of the Aral Sea Region. *The Eurasia Proceedings of Health, Environment and Life Sciences (EPHELS), 20,* 7-13.

The Eurasia Proceedings of Health, Environment and Life Sciences (EPHELS)
ISSN: 2791-8033

The Eurasia Proceedings of Health, Environment and Life Sciences (EPHELS), 2025

Volume 20, Pages 14-18

ICMeHeS 2025: International Conference on Medical and Health Sciences

In Vitro Micropropagation of Selected Halophytic Species from Family the *Chenopodiaceae (Amaranthaceae)*

Hulkar Khalbekova
Institute of Bioorganic Chemistry named after academician O. S. Sodiqov

Durdona Matchanova
Tashkent Chemical-Technological Institute

Abstract: This study focuses on the in vitro micropropagation of selected halophytic species belonging to the *Chenopodiaceae (Amaranthaceae*) family, collected from ecologically diverse and arid regions of Uzbekistan, including Sirdarya, Bukhara, and the drained Aral Sea zone (Muynak district). The primary objective was to establish sterile cultures, optimize the growth conditions, and evaluate the regenerative capacity and biomass accumulation of these salt-tolerant plants under controlled laboratory conditions.Sterile explants were obtained from seedlings germinated on Murashige and Skoog (MS) media supplemented with kinetin, BAP, or without growth regulators. Under these conditions, active germination was observed as early as days 3–6 of cultivation. The application of auxins and their combinations with kinetin, as well as 6-BAP—excluding media containing NAA - induced shoot regeneration across most annual halophyte species during both initial and subsequent subcultures. This led to a significant increase in explant proliferation and plant biomass production.For secondary subcultures of *Salsola dendroides, Salsola orientalis*, and *Salsola richteri*, Woody Plant Medium (WPM) was employed, demonstrating its suitability for maintaining and multiplying regenerants. The study highlights the effectiveness of specific plant growth regulators and media formulations in enhancing in vitro propagation efficiency.These results offer a promising foundation for the conservation, sustainable use, and possible reintroduction of halophytes into degraded saline environments, particularly the former Aral Sea bed. The established micropropagation protocols may further serve as a model for other stress-tolerant plant species with ecological and medicinal potential.

Keywords: In Vitro, Halophytes, Explant, Sterilization, Propagation.

Introduction

In the desert regions of Uzbekistan, the leading environmental stressors include an arid, sharply continental climate, high salinity levels in water and soil, pollution, and a shortage of potable water resources, as well as widespread desertification of formerly productive lands (Kamalov et al., 2001). These issues are particularly severe in the Aral Sea region, where the degradation of environmental conditions has been driven by a combination of natural and anthropogenic factors. This has led to a dramatic decline in sea levels and the frequent occurrence of dust and salt storms arising from the desiccated seabed.

Salinized soils are unsuitable for conventional agricultural crops, resulting in reduced productivity and economic losses in land management. However, certain promising halophytic species demonstrate high ecological adaptability and offer potential for the rehabilitation of saline lands and the establishment of specialized plantations. Halophytes serve as an important biological resource for agriculture, environmental restoration, and even medicinal applications (Waisel, 1972; O'Leary, 1985).

Many representatives of the *Chenopodiacea*e family are key edificators of halophytic vegetation in Uzbekistan. Modern scientific strategies for the sustainable use of plant resources in arid zones are closely linked to the development of plant biotechnology. In this context, the development of in vitro techniques for large-scale production of genetically stable microplants is of particular interest. This includes obtaining sterile and pathogen-free starting material suitable for regeneration and optimizing micropropagation conditions to promote shoot development and root system formation (Butenko, 1999).

Method

The study focused on long-vegetating halophytic species of the genera *Climacoptera, Atriplex, Suaeda, Halocnemum*, and various species of *Salsola*, collected in 2024 from the southern Aral Sea region, Republic of Karakalpakstan (Uzbekistan). To establish in vitro cultures, both seeds and seedlings were used as explants. The in vitro introduction process was divided into two main stages:

a) Sterilization (Decontamination): Plant material was treated with strong sterilizing agents to eliminate bacterial and fungal contamination and to obtain sterile explants.
b) Cultivation: The sterilized explants were cultured under standard in vitro conditions using agar-solidified nutrient media, following well-established protocols in plant biotechnology. At the end of each subculture (passage), the developmental responses of explants were recorded and analyzed (Dunaeva et al., 2017; Murashige & Skoog, 1962).

Results and Discussion

At the initial stage of disinfection, a 70% ethanol solution was applied for one minute. This was followed by the main phase of seed treatment, during which such parameters as reagent concentration and exposure time were optimized based on preliminary experiments. A variety of reagents were tested during the study, including Diacid, mercuric chloride, soap solutions, ethanol at different concentrations (70%, 75%, and 96%), and various dilutions of bleach solution (ratios of bleach to water: 1:10 and 1:20).

Significant results were achieved with a 0.001% solution of thimerosal applied for 30 minutes, treatment with 70% ethanol for 15–30 minutes, and triple rinsing with sterile distilled water after each treatment. This approach significantly increased the proportion of viable seeds. After the aseptic treatment phase, the solution was removed, and the seeds were carefully rinsed with sterile distilled water, further optimizing the percentage of seeds that retained viability (Khalbekova, 2023, 2024). Subsequently, the treated material was transferred onto a specified nutrient medium. Analysis of experimental results revealed that the proportion of plants free from endogenous microbial contamination varied depending on the species. Some species exhibited minimal internal microbial presence, resulting in a high percentage of sterile plants-ranging from 60% to 90%.

In this context, detailed optimization of growth regulator concentrations was conducted for in vitro cultures of plant species such as *Climacoptera, Atriplex, Suaeda, Halocnemum*, and *Salsola*. It is important to highlight that members of the Chenopodiaceae family showed a positive response to the introduction of growth stimulators. This effect was evident at the early stages of the cultivation process, significantly reducing the time between sowing and germination.

The emergence of the first seedlings in the studied species was observed within 7–15 days after sowing. After 28 days, the seedlings were transferred to fresh nutrient media. Cultivation of microcuttings on Murashige and Skoog (MS) medium led to the development of one to two shoots with elongated internodes, although the root systems were only weakly developed. Within 5–10 days after transferring explants to hormone-free MS medium, synchronous proliferation was observed.

For the first subculture, the optimal conditions were full-strength MS; for the second, ½ MS supplemented with 0.5 mg/L 6-benzylaminopurine (BAP) and 0.3 mg/L indole-3-butyric acid (IBA). To increase the number of regenerants, the following combinations were tested: ½ MS + 0.5 mg/L BAP + 0.5 mg/L kinetin (Kin) and ½ MS + 0.5 mg/L BAP + 0.3 mg/L IBA.

The stunted growth observed in seedlings from the Muynak region is likely due to their adaptation to extreme environmental conditions, which may result in lower nutrient demand during microshoot development. For the

continued growth of microshoots, a suitable medium was ½ MS supplemented with 0.5 mg/L BAP and 0.5 mg/L Kin, where the mortality rate of regenerants ranged from 12.1% to 28.7%.

Interestingly, optimal germination of aseptic seeds and formation of primary root systems in the studied species occurred under two conditions: ½ MS supplemented with 0.5 mg/L BAP + 0.3 mg/L IBA (60%) and hormone-free MS (90%). These media significantly stimulated in vitro seedling propagation. In contrast, species such as *Halocnemum* and *Salsola* required longer periods and higher hormone doses: initial shoot emergence was observed on day 10 after sowing, while complete leaf formation occurred within the next 7–10 days.

In vitro seed germination studies revealed low germination rates on media with various concentrations of the phytohormone Kin. However, when combined with the cytokinin BAP, both seed germination and seedling development were enhanced. Rooting of the initial explants typically began after 4–5 weeks. Under experimental conditions where the concentration of cytokinins exceeded that of auxins by 5–10 times, direct shoot formation was observed.

Callus Induction

To obtain sterile material, after treatment, the plant material was washed twice in distilled water and transferred directly to a nutrient environment. The seeds were transferred to a hormone-free environment with half salts MS (29) with sucrose with the addition of 7.5 g/l agar as a gel-forming component (Table 1).

Table 1. Efficiency of different culture media for in vitro regeneration of *Chenopodiaceae* species

№	Culture medium composition	Regeneration frequency (%)	Growth characteristics	Callus formation	Shoot formation	Overall efficiency
1	1	Full MS + 2 mg/L 6-BAP + 1 mg/L IAA	40%	Slow, elongated shoots	Moderate	Weak
2	2	MS + 1 mg/L 6-BAP + 0.5 mg/L NAA	55%	Moderate growth, thin shoots	Slight	Average
3	3	½ MS + 1 mg/L 6-BAP + 0.3 mg/L IAA + 2,4-D *(optimal)*	85%	Active growth, compact shoots	Controlled	**Good**
4	4	MS + 1.0 mg/L 2,4-D	30%	Callus without shoot development	Strong	None
5	5	½ MS without growth regulators *(control)*	10%	No morphogenesis	None	None

In the course of the experiment, seeds of the studied *Salsola* species were first cultivated in vitro. Then, several rectangular segments (0.2–0.5 mm) were excised from the central part of the leaf blade that had developed from the germinated seeds. These explants were placed on Murashige and Skoog (MS) medium supplemented with 0.5, 1.0, and 2.0 mg/L of the plant growth regulator 2,4-dichlorophenoxyacetic acid (2,4-D), with 10–12 leaf segments cultured per Petri dish. The cultures were incubated in darkness at 26 ± 2°C.

It was confirmed that the optimal concentration for callus induction and development from the leaves of *S. richteri and S. orientalis* was 0.5 mg/L 2,4-D when added to MS medium. The first hormonal responses of the explants were observed within one week. By the second week, soft whitish-yellow callus tissue had developed on media with MS + 0.5 mg/L 2,4-D. On media supplemented with MS + 0.5 mg/L 2,4-D + 0.3 mg/L 6-benzylaminopurine (BAP), relatively firm yellowish to light-green callus formed. Furthermore, improved callus quality was observed when the medium was supplemented with 0.5 mg/L 2,4-D + 0.3 mg/L BAP + 300 mM NaCl, which proved to be the most optimal formulation. Despite the taxonomic differences among the studied species, a shared biological characteristic in seed germination was noted. This pattern is also evident in the natural phytocenoses of these plants, which is likely attributable to their belonging to the same botanical family, *Chenopodiaceae*.

In particular, species of the genus Atriplex showed later stages of germination, with total germination rates ranging from 57% to 96%. On the other hand, species such as *Atriplex, Climacoptera, Chenopodium*, and *Suaeda*-despite morphological diversity ranging from shrubs to small trees like *Halocnemum* and *Salsola*-demonstrated a high germination capacity.

Under in vitro conditions, when using ½ MS + 0.5 mg/L 6-benzylaminopurine (BAP) + 0.3 mg/L indole-3-butyric acid (IBA) and hormone-free MS medium, seed germination efficiency ranged from 60% to 90%. It is assumed that the seeds of these species exhibit different dormancy stages, which depend not only on the species but also on the position of the seeds on the generative shoot.

When MS + 1.2 mg/L kinetin (Kin) + 0.1 mg/L IBA or ½ MS + 1 mg/L Kin + 0.1 mg/L IBA were used, all studied species showed low germination rates—from 8% to 15%. Such a combination of growth regulators had a negative effect on all halophytes: physiological processes slowed down, explant necrosis was observed, and root development was poor on media containing kinetin. Upon reducing the concentration of kinetin, an increase in seed germination was noted, reaching 10–12%, while root formation also reached 10%. When mature seeds were sown on media containing kinetin, they lost viability by the 14th day of cultivation.

For the induction of rhizogenesis in rooting experiments with all studied species of the *Chenopodiaceae* family, IBA at a concentration of 0.1 mg/L was shown to be optimal, with root induction ranging from 8% to 30%. However, increasing the IBA concentration to 0.3 mg/L improved rooting efficiency up to 97%. Nonetheless, at 0.1 mg/L IBA, roots appeared earlier and in greater numbers, making the concentration range of 0.1–0.3 mg/L IBA optimal for rhizogenesis in the studied halophytes.

It was noted that on such media, the seeds of all analyzed species demonstrated active germination rates between 30% and 60%. Interestingly, on hormone-free MS medium, the germination rate for all studied species was higher, reaching 70%–80%. After 10 days of cultivation on MS medium without hormone supplements, seed germination reached an impressive 97%. In contrast, when the same seeds were placed on media containing kinetin, germination dropped to just 12%.

Shoot Regeneration

Shoot regeneration from callus was successfully achieved by transferring callus to MS medium supplemented with 1.0 mg/L BAP and 0.5 mg/L indole-3-acetic acid (IAA). The maximum regeneration rate (60%) was recorded 21 days after the callus was transferred to the regeneration medium. The developed in vitro propagation protocol for Salsola species enables the efficient production of sterile plants, callus, and regenerated shoots. Notably, successful seed sterilization proved to be a critical step, directly influencing the viability of the resulting seedlings. The high percentage of regenerants obtained following sterilization confirms the preservation of tissue physiological activity and the successful initiation of morphogenesis.

Conclusion

Thus, as a result of the conducted studies, it was determined that seeds of the studied halophyte species from the Chenopodiaceae family, when placed on media supplemented with kinetin, as well as on media containing BAP or MS without hormones, germinated actively within 3 to 6 days of cultivation. The applied auxins and their combinations with kinetin, as well as BAP (with the exception of the medium containing NAA), induced the formation of regenerants during both the initial and subsequent subcultures in all annual halophyte species, leading to an increase in the number of explants. For the secondary subcultures of Salsola dendroides, Salsola orientalis, and Salsola richteri, the ready-made WPM medium was used.

Scientific Ethics Declaration

* The authors declare that the scientific ethical and legal responsibility of this article published in EPHELS journal belongs to the authors.

Conflicts of Interest

* The authors declare no conflict of interest.

Funding

* This research received no specific grant from any funding agency in the public, commercial, or not-for-profit sectors.

Acknowledgements or Notes

* This article was presented as a poster presentation at the International Conference on Medical and Health Sciences (www.icmehes.net) held in Antalya/Türkiye on November 12-15, 2025.

References

Butenko, R. G. (1999). *Biology of higher plant cells in vitro and biotechnology based on them* (p. 160). Moscow: FBK-Press.

Dunaeva, S. E., Pendinen, G. I., Antonova, O. Yu., Shchvachko, I. I., Ukhatova, Yu. V., Shuvalova, L. E., Volkova, N. N., & Gavrshenko, T. A. (2017). *Conservation of vegetatively propagated crops in in vitro and cryo collections: Methodological guidelines* (pp. 70–71). St. Petersburg: VIR.

Kamalov, Sh., Ashurmetov, O. A., & Bakhiev, A. B. (2001). Some results of phytomelioration of saline soils in the southern part of the dried bottom of the Aral Sea and the Aral Sea region. *Bulletin of the Karakalpak Branch of the Academy of Sciences of the Republic of Uzbekistan*, *6*, 3–6.

Khalbekova, H. U. (2023). Amino acid composition of species of the genus *Atriplex* L. growing in the Aral Sea (Uzbekistan). In *VI International Conference on Actual Problems of the Energy Complex and Environmental Protection*, *411*, 1–5.

Khalbekova, H. U. (2024). Adaptive and viable characteristics of microclonal seedlings of hyperhylophyte *Suaeda arcuata* under in vitro conditions. In *III International Conference on Agriculture, Earth Remote Sensing and Environment*, *539*, 1–7.

Murashige, T., & Skoog, F. A. (1962). A revised medium for rapid growth and bio-assays with tobacco tissue cultures. *Physiologia Plantarum*, *15*(3), 473–497.

O'Leary, I. (1985). Halophytes. *Arizona Land and People*, *30*(30), 15–16.

Waisel, Y. (1972). *Biology of halophytes* (p. 395). New York, NY: Academic Press.

Author(s) Information

Hulkar Khalbekova
Institute of Bioorganic Chemistry named after academician O. S. Sodiqov
Mirzo Ulugbek Avenue, 83, Tashkent, 100125, Republic of Uzbekistan.
Contact e-mail: *xalbekova.xulkar@bk.ru*

Durdona Matchanova
Tashkent Chemical-Technological Institute
Navoiy Avenue, 32, Tashkent,100011,
Republic of Uzbekistan.

To cite this article:

Khalbekova H., & Matchanova D. (2025). In vitro micropropagation of selected halophytic species from family the *Chenopodiaceae (Amaranthaceae*). *The Eurasia Proceedings of Health, Environment and Life Sciences (EPHELS), 20,* 14-18.

The Eurasia Proceedings of Health, Environment and Life Sciences (EPHELS)
ISSN: 2791-8033

The Eurasia Proceedings of Health, Environment and Life Sciences (EPHELS), 2025

Volume 20, Pages 19-31

ICMeHeS 2025: International Conference on Medical and Health Sciences

Cytotoxic and Antiproliferative Activities of Nymphaea Lotus and 5-Fluorouracil on Ehrlich Ascites Carcinoma Cells

Ridwan Lawal
University of Lagos

Mehmet Ozaslan
Gaziantep University

Dayo Adedoyin
Yaba College of Technology

Obumneme Patrick Okoye
University of Lagos

Abstract: *Nymphaea lotus* Linn (Nymphaeceae), an ubiquitious tropical water plant is a major component of herbal decoctions administered in rural Nigeria for the treatment of a wide range of diseases including cancers. However, the potency and mechanism of antiproliferative action of the plant extract against tumours are not yet established. This study was designed to investigate *in vivo* and *in vitro* the anti-tumour potency of ethanol extract of *Nymphaea lotus* (NLE) in comparison with 5-fluorouracil (Standard anti-tumour drug) in EAC-treated Swiss albino mice. 20 acclimatized adult male Swiss albino mice were inoculated with 10^6 EAC cells/mouse *intraperitoneally* and randomly divided into 4 groups of 5 mice/group. Group I served as negative control (EAC only), groups II and III received *intraperitoneal* injections of 20 and 40 mg/kg bodyweight NLE for 14 days while Group IV received 20 mg/kg fluorouracil. A fifth group of 5 mice served as the baseline control and was administered only 0.9% NaCl (Physiological saline). Tumour development was evaluated by determining the weight gain, ascitic weight gain and volume. MST and percentage ILS were also determined. DNA was extracted from EAC cells from treated animals and subjected to DNA fragmentation assay via electrophoresis. *Intraperitoneal* administration of 40 mg/kg bodyweight NLE significantly reduced the ascetic fluid volume, induced morphological changes, decreased the viability of the ascitic cells and also caused a prolongation of the lifespan of animals. *Nymphaea lotus* elicited similar pattern of responses to 5-fluorouracil which are characteristic of apoptosis.

Keywords: Ehrlich, Apoptotic, *Nymphaea lotus*, Intraperitoneal, Tumour, Fluorouracil

Introduction

Nymphaea lotus Linn (Nymphaeaceae) is a water plant generally found in Tropical and Sub-Saharan Africa. The leaves are mostly green and found floating with a spreading perianth. Compounds such as amino butanoic acid, Serine-arginine dipeptide, Tyrosine, 2-amino-7-methyl octanoic acid have been reportedly isolated from the plant (Sowemimo et al., 2007a). Its cytotoxic activity as well as telomerase inhibitory activity has also been reported (Sowemimo et al., 2007b) lending credence to its ethnomedicinal use in cancer treatment. This study was aimed at assessing the role of *Nymphaea lotus* in inhibiting Ehrlich Ascites Carcinoma in male Swiss albino mice.

Method

Materials and Methods

Trypan blue was from Bio-tech Pvt Ltd (India), 5-Fluorouracil from KOCAK FARMA (TURKEY) was used as a standard drug based on previous literature significantly enhanced the life span in EAC tumors (Muthuraman et al., 2008). All other chemicals used were of analytical grade available locally.

Plant Collection

Nymphaea lotus whole plant was collected from Osogbo, South-West, Nigeria. Plant material was identified by Mr Odewo. A voucher specimen was deposited in the University Herbarium, University of Lagos, Lagos, Nigeria with voucher number: LUH 3493.

Preparation of Aqueous Extract

The plant materials were shade dried for 3 days and pulverized into powder. Ethanol extract of the coarsely powdered material was prepared by macerating 1kg of whole plant in 1 L of distilled water for 72 hours. The marcerate was filtered and the filtrate was concentrated using the Rotary Evaporator and further concentrated to constant weight *in vacuo* using a lyotrap.

In-vitro EAC Cell Culture

Ten days after inoculation of EAT cells in the abdominal cavity of mice, the cells were isolated by needle aspiration, washed in saline, and the erythrocytes removed with a lysing solution. Ascitic tumour cell counts are done in a Cell Counting machine (Cedex, Roche) using the trypan blue dye exclusion method. Cell viability was > 95%. Tumour cell suspensions were prepared in phosphate balanced salt solution (PBS) at pH 7.4 to final concentrations of 1×10^6 viable cells ml^{-1} (Ozaslan et al., 2010).

In-vitro Cytotoxicity

In vitro cytotoxic activity was carried out using the Trypan Blue dye exclusion method. Briefly, aqueous extract of *Nymphaea lotus* in Phosphate buffered saline (1000, 100, 10, 1 and 0.1 µg/ml) were incubated with EAC cells at 37^0C. Ascitic tumour cell counts were done in a Cell Counting machine (Cedex, Roche) using the trypan blue dye exclusion method. Results were expressed as Percentage Cell viability (Saluja et al., 2011).

Animals

Adult Swiss male albino mice (26-33 g) were procured from University of Gaziantep, Turkey and used throughout the study. They were housed in prophylene cages in a controlled environment (temperature 25±2°C and 12 h dark and light cycle) with standard diet and water *ad libitum*. The animal experiments were carried out in accordance with the Institutional Protocols of Animal Care. The study was conducted after obtaining institutional animal ethic committee clearance of the University of Gaziantep, Gaziantep, Turkey.

EAC Cell Culture

Ehrlich Ascites Carcinoma cells were procured from Professor (Dr.) Mehmet Ozaslan, Department of Biology, University of Gaziantep, Turkey. They were grown by weekly *intra peritoneal* inoculation of 10^6 cells/mouse according to the method of Lawal et al. (2012). The tumour cell counts of the Ehrlich ascites cells were conducted using an automated Cell Counter (Cedex, Roche) and the trypan blue dye exclusion method.

Ehrlich ascites cells with viability above 95% were selected for the experiment. The tumour cell suspensions were prepared in phosphate balanced salt solution (PBS) at pH 7.4 to final concentrations of 1×10^6 viable cells

ml^{-1}. The mice were given *intra peritoneal* (i.p.) injection of 1×10^6 viable tumour cells per mouse in a volume of 0.2 ml according to the method of Justo et al. (2000).

In-vivo Study

Animals were inoculated with 1 x 10^6 cells/mouse on day '0' and treatment with *intra peritoneal Nymphaea lotus* extract started 24 h after inoculation, at a dose of 10, 20 and 40 mg/kg/day. The control group were treated with same volume of 0.9% sodium chloride solution. All the treatments were given for 14 days. Mortality was recorded daily. The mean survival time (MST) of each group, consisting of 5 mice was noted. The antitumor efficacy of SLE was compared with that of 5-fluorouracil (5-FU, 20 mg/kg/day, *i.p* for 14 days). The effect of NL on percentage increase in life span was calculated on the basis of mortality of the experimental mice (Sur and Ganguly, 1994). Mean survival time and Increased Life Span (% ILS) was calculated using the following equation (Mazumder et al., 1997; Gupta et al., 2000):

$$\text{MST} = \frac{\sum \text{Survival time (days) of each mouse in a group}}{\text{Total number of mice}}$$

$$\text{ILS} = \frac{\text{MST of treated group}}{\text{MST of control group}} \times 100$$

Antitumor Activity

Male Swiss albino mice are divided into 6 groups (n = 5). All the groups were injected with EAC cells (0.2 ml of $1x10^6$ cells/mouse) intraperitoneally (Gupta *et al.,* 2004) except Group I. This was taken as day Zero. Twenty (24) hours after inoculation, animals start receiving daily *intra peritoneal* administration of different concentration of *Nymphaea lotus* extract.

Group I - Normal control.
Group II - Disease Control, EAC cell line ($1x10^6$ cell mouse).
Group III - EAC cell line ($1x10^6$ cells) treated with 40 mg/kg i.p NLE.
Group IV - EAC cell line ($1x10^6$ cells) treated with standard [5- flurouracil (20 mg/kg i.p.)]

After 14 days of treatment, animals from each group were sacrificed by ether anesthesia. The total number of tumour cells in the peritoneal cavity was counted by the trypan blue exclusion method (Bromberg et al., 2012) using the Cedex counter (Kavimani & Manisenthil kumar, 2000).

Ascite Volume

The ascitic fluid from the peritoneal cavity of tumour bearing mice was quantitatively isolated by peritoneal lavage after death into graduated eppendorf tubes and measured (Prakash et al., 2011).

Ascite Weight

The mice were dissected for collecting ascitic fluid from peritoneal cavity. The ascetic fluid was carefully collected with the help of 5 mL sterile syringe into pre-weighed eppendorf tubes. The ascite weight was calculated using the formula;

$$\text{Ascite Weight} = \text{Final Weight of Eppendorf} - \text{Weight of pre-weighed eppendorf}$$

Ehrlich Packed Cell Volume

The mice were carefully dissected in order to collect the ascitic fluid from peritoneal cavity. One ml of the ascite fluid of the transplantable murine tumor was carefully collected with the help of 5 mL sterile syringe. The fluid was subsequently transferred to a graduated glass centrifuge tube and centrifuged at 1000 rpm for 5 min. The fluid volume was measured. Ehrlich packed cell volume was determined using the following formula;

$$\text{Ehrlich Packed Cell volume (\%)} = \frac{\text{1- volume of fluid}}{1} \times 100$$

Blood Packed Cell Volume

One ml of blood was obtained from each mouse via left ventricular cardiac puncture and was centrifuged at 2500 rpm for 10 minutes. The Packed Cell volume was calculated by using the following formula;

$$\text{Blood PCV (\%)} = \frac{\text{1 – volume of liquid}}{1} \times 100$$

DNA Isolation from Ehrlich Ascites Carcinoma Cells

The EAC cells collected from treated and untreated animals were used for DNA fragmentation assay using the modified method of Jun-ya UEDA et al. (2002) as described briefly. Cells were washed twice in 800 µL of PBS and pelleted. Pelleted cells were lysed in 600 µL of Lysis buffer (10 mM Tris-HCl buffer, pH 8.0, 10 mM EDTA and 0.2% Triton X-100) for 10 minutes on ice. The lysate was centrifuged at 6000 rpm for 20 mins. The supernatant was then extracted with 1000 µL of PCIAA (Phenol – chloroform - Isoamylalcohol solution, 25:24:1). The mixture was then centrifuged at 6000rpm for 20 mins and the upper layer decanted off and precipitated with 50 µL of 3M NaCl and 1000 µL of cold ethanol at -20^0C overnight. After drying, the isolated DNA was dissolved in TE buffer. Contamination by RNA was eliminated by incubation with 40 units of RNase at 37^0C for 30 minutes.

DNA Fragmentation Assay On 2% Agarose Gel

Loading buffer was added, and (fragmented) DNA electrophoresed on 2% agarose gel in TBE (40 mM Tris, 20 mM Boric acid, 1mM EDTA) at 100 V for 45 minutes and visualized by EtBr staining.

Statistical Analysis

Results are expressed as Mean ± S.E.M., SPSS package was used for data analysis and t-test was used for determining the significance ($P<0.05$) between mean values within a group.

Results and Discussion

In- vitro cytotoxicity study indicates that the aqueous extract of *Nymphaea lotus* had a dose-dependent cytotoxic effect on EAC cells *in-vitro* (Table 1).

Table 1. *In vitro* cytotoxic effect of Aqueous extracts of *Nymphaea lotus* on Ehrlich Ascites Carcinoma cells.

Concentration (µg/ml)	Mortality
1000	40.8
100	39.6
10	7.8
1	5.8
0.1	-

*Results are expressed as Mean of 3 determinations

IC_{50} value of 2691µg/ml was calculated using Probit analysis

Administration of 40 mg/kg *Nymphaea lotus* led to a significant reduction in body weight as compared to EAC tumour-bearing mice. 5-fluorouracil also caused a significant reduction in bodyweight of tumour-bearing mice (Figure 1).

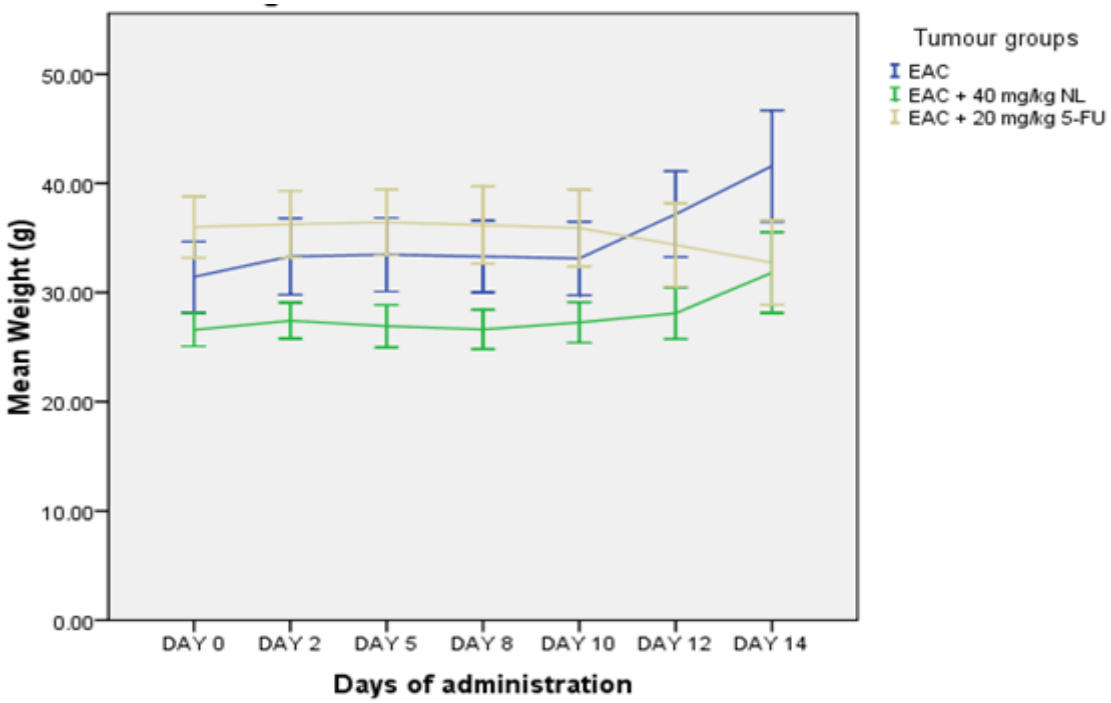

Figure 1. Effect of administration of 10 mg/kg body-weight *Nymphaea lotus* and 20 mg/kg body-weight 5-fluorouracil on the body weight of tumour bearing-mice

The effect of NLE on the survival of tumour-bearing mice is shown in Table 2. The Mean Survival time (MST) for the control group was 14.4 days whereas MST was 14.0, 14.6 and 17.4 days respectively for the groups treated with 20, 40 mg/kg bodyweight NLE and 20 mg/kg bodyweight 5-fluorouracil respectively. The percentage increase in life span of tumour-bearing mice treated with 20, 40 mg/kg NLE and 20 mg/kg 5-fluorouracil was found to be -2.7, 1.4 and 21% respectively as compared to the diseased control (Table 2).

Table 2. Mean survival time and increased life span of Ehrlich ascites-bearing mice treated with *Nymphaea lotus* extract and 5-fluorouracil*

Groups	Treatment	MST (days)	ILS (%)
1	EAC + Normal Saline	14.40 ± 0.93	-
2	EAC +20 mg/kg b.wt NL	14.00 ± 2.07	-2.7
3	EAC +40 mg/kg b.wt NL	14.60 ± 1.21	1.4
4	EAC +20 mg/kg b.wt 5-FU	17.40 ± 1.91	20.8

*Results are expressed as Mean ± Standard error of mean (S.E.M)
Values with different superscripts are significantly different from control

Reports have shown that the trypan blue assay as well as other direct cell counting methods, give more accurate results compared to other assays which take into account the metabolism of the cells (Hanaske, 1993). Saluja et al. (2011) reported that *Madhuca longifolia* leaves ethanolic extract at a concentration of 200µg/ml showed 84% activity while acetone extract caused 78% activity using the trypan blue assay. The trypan blue exclusion assay takes advantage of the ability of healthy cells with uncompromised cytoplasmic membrane integrity to exclude the dye, trypan blue. Dead cells are selectively stained and healthy cells can be counted directly using the method of Tran et al. (2011).

According to the US NCI plant screening programme, crude extracts are generally considered to have *in vitro* cytotoxic activity if the IC_{50} value (concentration that causes a 50% cell kill) in carcinoma cells, following incubation between 48 and 72 hours, is less than 20 µg/ml, while it is less than 4 µg/ml for pure compounds (Boik et al., 2001). The high IC_{50} in this research were recorded after a short-term exposure to the extract. An increased/ long term exposure to the extract could have led to a cell kill of less than the value recorded in this study.

Table 3. Effect of *Nymphaea lotus* and 5-fluorouracil on viability of Ehrlich Ascites carcinoma cells in tumour-bearing mice*

Groups	EAC only	EAC + 20 mg/kg FU	EAC + 40 mg/kg NL
Viable Cell Count	1091 ± 11.61[a]	153.33 ± 18.49[b]	814.33 ± 267.23[a]
Dead Cell Count	413.67 ± 14.49[a]	537.33 ± 39.18[a]	4354.33 ± 291.87[b]
Total Cell Count	1505 ± 2.91[a]	690.67 ± 25.95[a]	5168.67 ± 552.61[b]
Total Cell Concentration ($\times 10^5$) (cells/ml)	423.81 ± 3.43 [a]	175.16 ± 5.14[a]	718.17 ± 76.78[b]
Viability (%)	72.46 ± 0.91[a]	22.30 ± 3.30[b]	15.07 ± 3.25[b]

*Results are expressed as Mean ± Standard error of mean (S.E.M)
Values with different superscripts are significantly different from control

Ehrlich ascites carcinoma (EAC) cells as a model in anticancer research has been proven by many authors (Clarkson & Burchenal, 1965; Prakash et al., 2011) to give accurate and reliable results as we have shown also in our previous studies. The reliability of such test lies in their ability to determine the value of any anti-cancer drug through the prolongation of experimental animals' life span in addition to changes in number and viability of the cell line itself in addition to the volume of the liquid generated by the tumour inside the peritoneal cavity (Maity et al., 1999). NL was able to elongate the life span of EAC-bearing mice. Adreani *et al.*, 1983 had suggested that an increased life span of ascites-bearing animals by 25% is considered to be an indicator of significant drug activity.

Doses of 40 mg/kg *Nymphaea lotus* when administered showed a lower ability to cause elongation of life span compared to 20 mg/kg 5-fluorouracil. 5-fluorouracil has been shown to significantly enhance the lifespan in EAC tumors (Fodstat et al., 1977) and was used as the reference drug in this study. In a previous study by Muthuraman *et al.* (2008), 100 mg/kg of *Tragia plukenetti* caused an ILS of 29.41 while fluorouracil caused an ILS of 92.88%. In this study, dose of 40 mg/kg of NL showed a lower ability to cause elongation of lifespan when compared to 5-fluoruracil (Table 2). Biswas *et al.* (2010) suggested that prevention of tumour progression by bioactive agents in medicinal plants may be responsible for the increase in lifespan observed.

In vivo, the extract was able to exert its cytotoxic effect by reducing the viable cell count when administered. This was in accordance with the findings of other researchers (Prakash et al., 2011). The increased life span reported earlier could be attributed to the reduction in the viable cell count, hence a decrease in the tumour burden. The efficacy of the extract or the reference drug is demonstrated by an ability to cause a reduction in the weight of the animals when compared to a diseased animal (Muthuraman et al., 2008). The changes in body weight monitored throughout the period of the experiment indicated a percentage decrease in the weight after administration of extract to EAC-induced animals.

The changes observed in NL-administered animals were different from those obtained when the reference drug was used. The percentage decrease in mean Ehrlich ascites weight recorded as a result of the cytotoxic effect of the extract could be responsible for the reduction in weight of animals. The standard drug, fluorouracil gave a similar response though the extract showed more potency in causing a reduction in weight. Ahmed et al. (1988) studied the interaction and *in vivo* growth inhibition of EAC cells by Jacalin. They observed that mice given an injection of EAC only had an average weight gain of 6.9 g one week after inoculation. This increase in body-weight was ascribed to accumulation of ascites fluid of EAC. However, they observed that mice receiving Jacalin (which was cytotoxic to EAC) showed a weight gain of 1.2 - 2 g after the same period.

The mean Ehrlich ascites volume, weight and Packed cell volume are used as measures of tumour growth response (Biswas et al., 2010; Prakash et al., 2011). The reduction in intraperitoneal tumour burden observed after administration of extract may be due to the cytotoxic agents present in the extract which prevent tumour progression by killing cells through the lysis of the cell membrane. The findings of this work are similar to the report of Biswas et al., 2010 in which *Dregen volubilis* fruit showed strong antitumour effect in EAC-bearing mice by causing a reduction in tumour volume, weight and viable cell count in a dose-dependent manner. In order to ensure that these malignant cells receive the nourishment they need to thrive, angiogenesis which is the formation of new blood vessels occurs (Yarbro et al., 2005). Angiogenesis has been reported to be one of the factors responsible for the accumulation of ascites fluid in the peritoneal cavity of tumour-bearing mice (Badr et al., 2011). The progressive ascitic fluid formation due to implantation of EAC causes an increasing vascular permeability due to a rise in VEGF (Fecchio et al., 1990). The reduction in EAC tumor volume may be due to a reduced expression of VEGF by the administration of extract leading to a decreased angiogenesis.

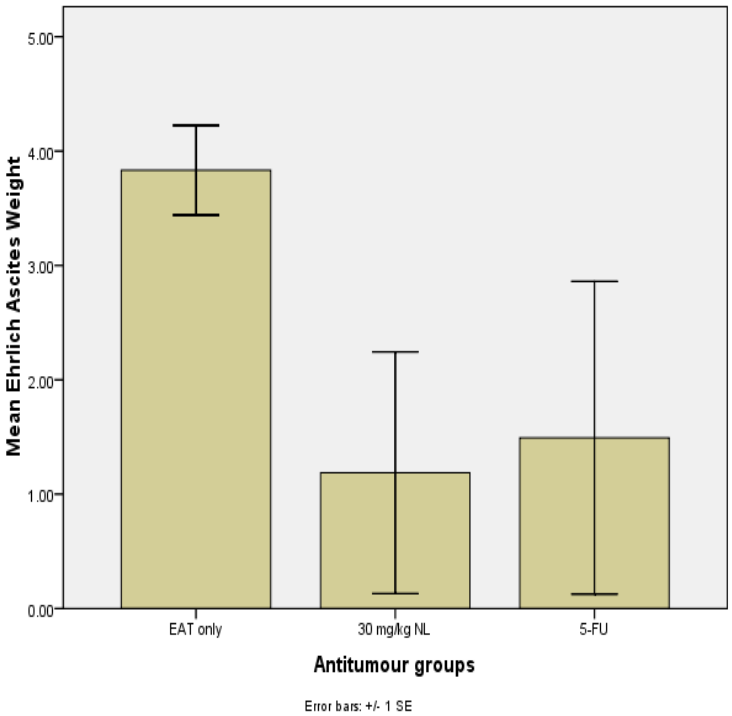

Figure 2. Effect of *Nymphaea lotus* and 5-fluorouracil on weight of Ehrlich Ascites carcinoma cells in tumour-bearing mice.
*Values are significantly different from control (P<0.05)
Keys: 5-FU (5-fluorouracil), EAC (Ehrlich ascites carcinoma). NL - *Nymphaea lotus*

Packed cell volume describes the volume that is occupied by a cell pellet after centrifugation. The % PCV value linearly correlates with the cell density. The blood packed cell volume is the volume of the cells expressed as a percentage of total blood volume (Nowak & Handford, 1994).

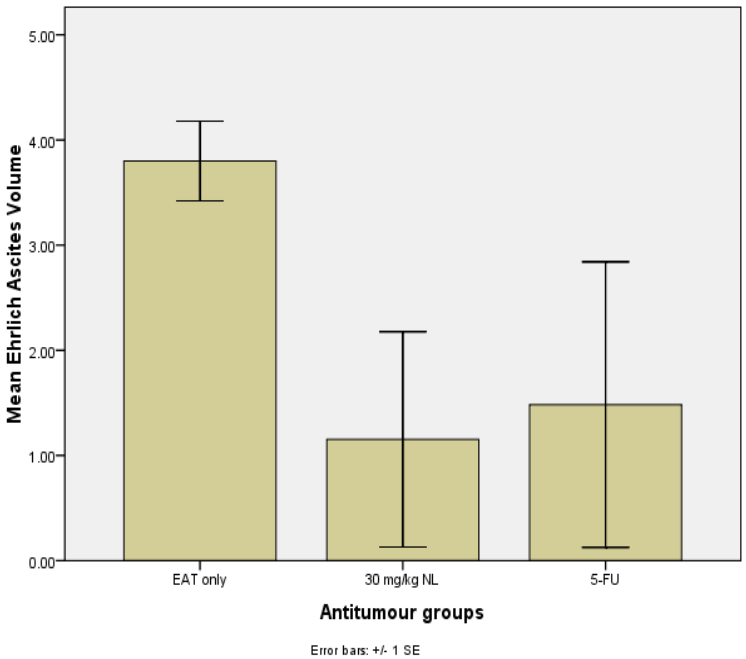

Figure 3. Effect of administration of 10 mg/kg body-weight *Nymphaea lotus* and 20 mg/kg body-weight 5-fluorouracil on Mean EAC volume of tumour bearing-mice.
*Results are expressed as Mean ± Standard error of mean (S.E.M)
Values with different superscripts are significantly different from control
EAC – Ehrlich ascites carcinoma cells, NL – *Nymphaea lotus*, 5-FU – 5-fluorouracil

The decreased Ehrlich packed cell volume observed in this experiment further shows that cytotoxic agents such as saponins present in the extract may be involved in cell lysis and hence caused a decreased percentage of viable cells. The response of EAC cells to NL *in vitro* corresponds to the behaviour *in vivo.*

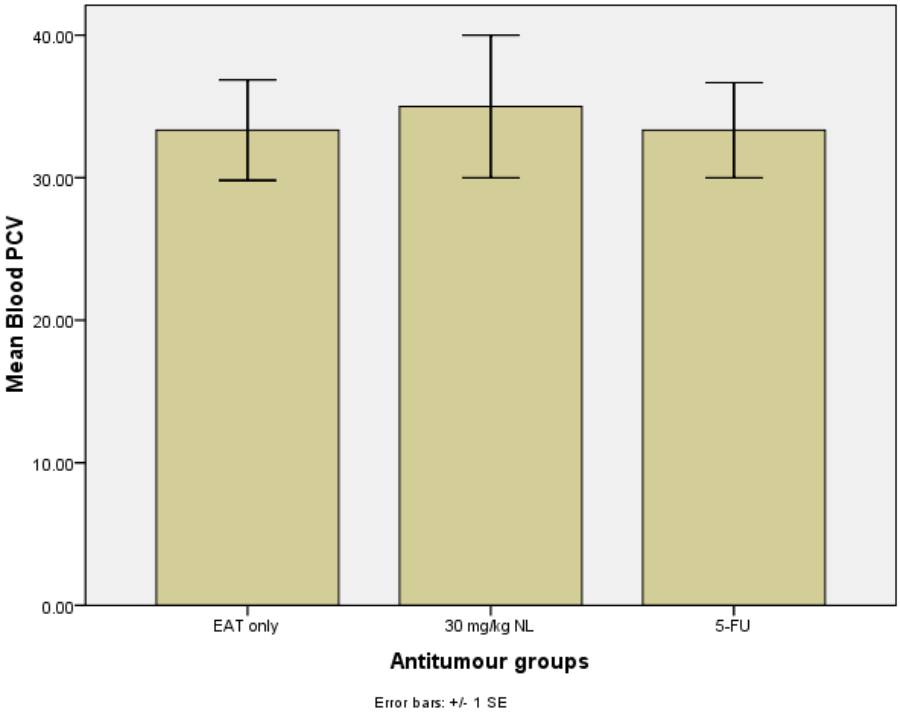

Figure 4. Effect of *Nymphaea lotus* and 5-fluorouracil on Blood PCV of tumour-bearing mice.
*Values are significantly different from control (P<0.05)
5-FU (5-fluorouracil), EAT (Ehrlich ascites carcinoma cells). NL - *Nymphaea lotus*

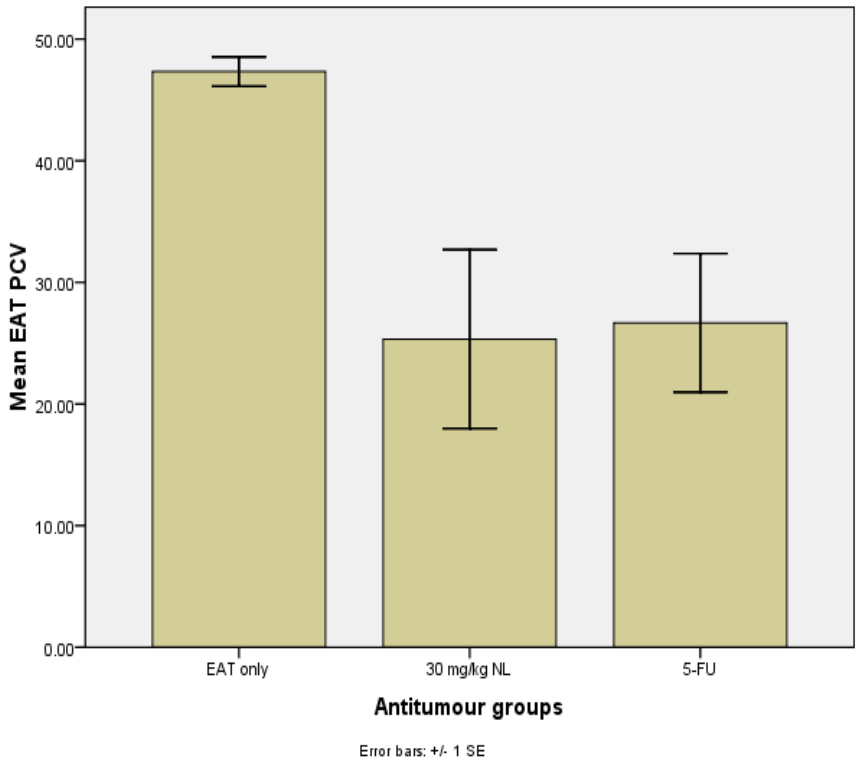

Figure 5. Effect of *Nymphaea lotus* and 5-fluorouracil on EAC PCV of Ehrlich Ascites carcinoma cells in tumour-bearing mice.
*Values are significantly different from control (P<0.05)
Keys: 5-FU (5-fluorouracil), EAT (Ehrlich ascites carcinoma cells). NL - *Nymphaea lotus*

Apoptotic cells are characterised by a number of structural and morphological features such as cell shrinkage, membrane blebbing, chromatin condensation and the formation of apoptotic bodies (Zimmerman et al., 2001; Orienius, 2004).

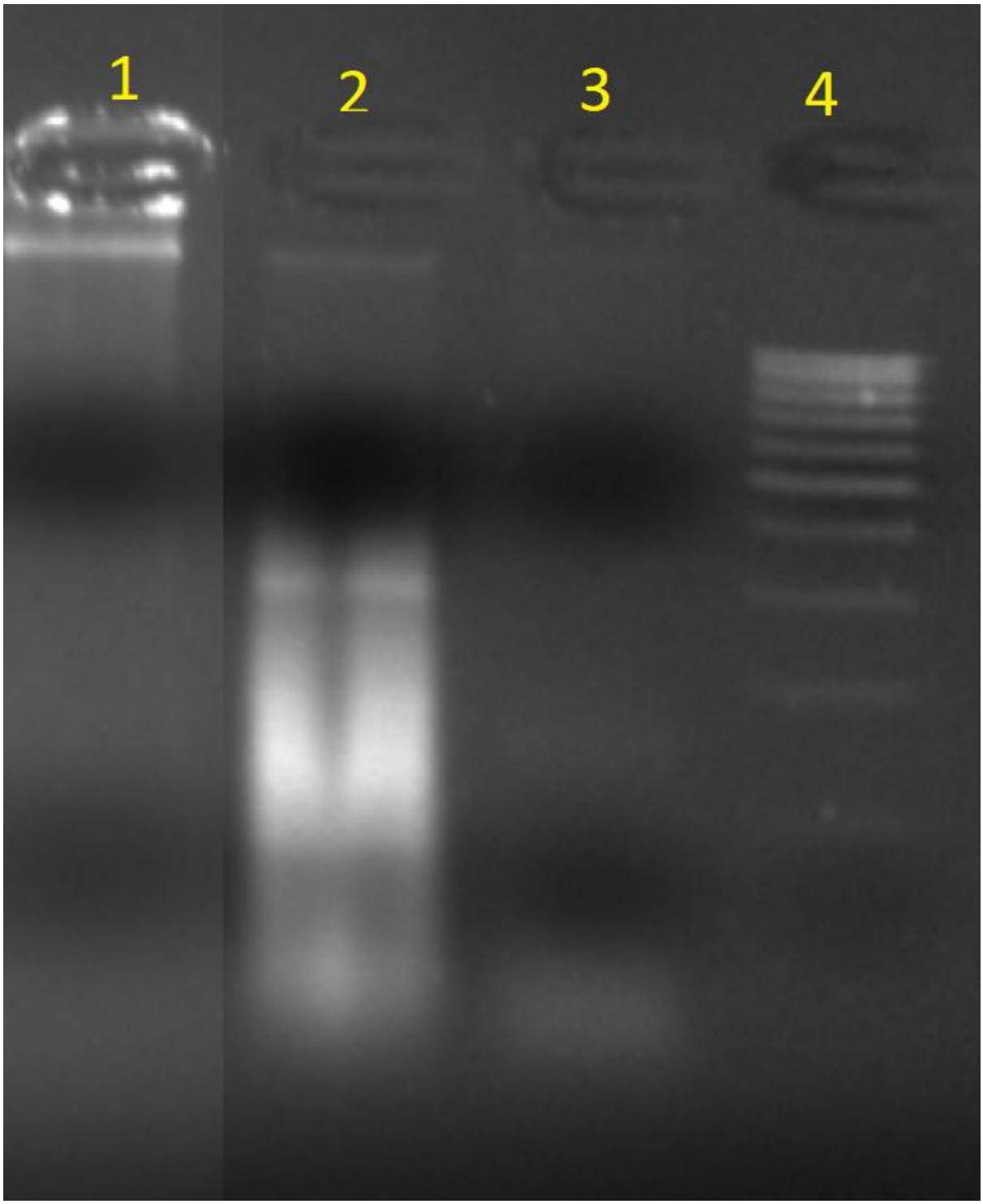

Figure 6. The aqueous extract of *Nymphaea lotus* from Osogbo, Nigeria induced DNA fragmentation in Ehrlich ascites carcinoma comparable to the effect of 5-fluorouracil. Lane 1- EAC control, Lane 2- EAC + NL extract, Lane 3- EAC + fluorouracil, Lane 4- DNA laddeer (marker).

The extract inhibited the growth of tumour cells and induced morphological changes typical of apoptosis. Results of the DNA fragmentation assay indicated that the ethanol extract of *Nymphaea lotus* induced ladder-like DNA fragmentation. The presence of this ladder has been extensively used as a marker for apoptotic cell

death (Wyllie, 1980; Nagata, 2000). However, further studies are needed for better understanding of how NL activated apoptotic cascade.

Conclusion

Nymphaea lotus showed potent cytotoxic and antiproliferative activities of *Nymphaea lotus* on Ehrlich ascites carcinoma cells which was comparable to that of 5-fluorouracil, a standard anti-cancer drug.

Recommendations

Further studies can be done to isolate and identify phytochemicals with cytotoxic and antiproliferative activity.

Scientific Ethics Declaration

* The authors declare that the scientific ethical and legal responsibility of this article published in EPHELS journal belongs to the authors.

Conflicts of Interest

* The authors declare no conflict of interest.

Funding

* This research received no specific grant from any funding agency in the public, commercial, or not-for-profit sectors.

Acknowledgements or Notes

* This article was presented as an oral presentation at the International Conference on Medical and Health Sciences (www.icmehes.net) held in Antalya/Türkiye on November 12-15, 2025.

References

Abdullaev, F. I., Luna, R. R., Roitenburd, B. V., & Espinosa, A. J. (2000). Pattern of childhood cancer mortality in Mexico. *Archives of Medical Research, 31*, 526–531.

Adreani, A., Scapini, G., & Galatulas, I. (1983). Potential antitumor agents IX: Synthesis and antitumor activity of two analogues of ketocaine. *Journal of Pharmaceutical Sciences, 72*, 814–819.

Agrawal, S. S., Saraswati, S., Mathur, R., & Pandey, M. (2011). Antitumor properties of Boswellic acid against Ehrlich ascites cells bearing mouse. *Food and Chemical Toxicology, 49*, 1924–1934.

Agrawala, S. K., Chatterjee, S., & Misra, S. K. (2001**).** Immune-potentiation activity of a polyherbal formulation 'Immu-21'. *Phytomedica, 2*, 1–22.

Ahmed, H., Chatterjee, B. P., & Debnath, A. K. (1988). Interaction and in vivo growth inhibition of Ehrlich ascites tumour cells by jacalin. *Journal of Biosciences, 13*(4), 419–424.

Badr, M. O. T., Edrees, N. M. M., Amany, A. M. A., Nasr, A. M. N., Ahmed, N. F. N., & Hager, T. H. I. (2011). Anti-tumour effects of Egyptian propolis on Ehrlich ascites carcinoma. *Veterinaria Italiana, 47*(3), 341–350.

Bhattacharyya, A., Mandal, D., Lahiry, L., Sa, G., & Das, T. (2004**).** Black tea protects immunocytes from tumor-induced apoptosis by changing Bcl-2/Bax ratio. *Cancer Letters, 209*, 147–154.

Biswas, M., Bera, S., Kar, B., Karan, T. K., Bhattacharya, S., Ghosh, A. K., & Haldar, P. K. (2010). Antitumour effect of *Dregea volubilis* fruit in Ehrlich ascites carcinoma-bearing mice. *Global Journal of Pharmacology, 4*(3), 102–106.

Boik, J. (2001). *Natural compounds in cancer therapy.* Oregon Medical Press.

Bredow, J., Kretzschmar, M., Wunderlich, G., Dörr, W., Pohl, T., Franke, W. G., & Kotzerke, J. (2004). Therapy of malignant ascites in vivo by 211At-labelled microspheres. *Nuklearmedizin, 43*, 63–68.

Bromberg, N., Dreyfuss, J. L., Regatieri, C. V., Palladino, M. V., Durán, N., …& Nader, H. B. (2010). Growth inhibition and pro-apoptotic activity of violacein in Ehrlich ascites tumor. *Chemico-Biological Interactions, 186*, 43–52.

Burkill, H. M. (1997). *The useful plants of West Africa* (Vol. 4). Royal Botanic Gardens, Kew.

Christou, L., Hatzimichael, E., Chaidos, A., Tsiara, S., & Bourantas, K. L. (2001). Treatment of plasma cell leukemia with vincristine, liposomal doxorubicin and dexamethasone. *European Journal of Haematology, 67*, 51–53.

Clarkson, B. D., & Burchenal, J. H. (1965). Preliminary screening of antineoplastic drugs. *Progress in Clinical Cancer, 1*, 625–629.

Corner, J. (2001). What is cancer? In J. Corner & C. Bailey (Eds.), *Cancer nursing: Care in context*. Blackwell Publishing.

Cragg, G. M., & Newman, D. J. (2005). Plants as a source of anti-cancer agents. *Journal of Ethnopharmacology, 100*, 72–79.

Denault, J. B., & Salvesen, G. S. (2002). Caspases: Keys in the ignition of cell death. *Chemical Reviews, 102*(12), 4489–4500.

Dongre, S. H., Badami, S., Natesan, S., & Chandrashekhar, R. H. (2007). Antitumor activity of the methanol extract of *Hypericum hookerianum* stem against Ehrlich ascites carcinoma in Swiss albino mice. *Journal of Pharmacological Sciences, 103*, 354–359.

Fodstad, Ø., Olsnes, S., & Alexander, P. A. (1977). Inhibitory effect of abrin and ricin on transplantable murine tumors and human cancers in nude mice. *Cancer Research, 37*, 4559–4567.

Goldie, H. (1956). Growth characteristics of free tumour cells in various body fluids and tissues of the mouse. *Annals of the New York Academy of Sciences, 63*, 711–727.

Gupta, A., Mazumder, U. K., Kumar, R. S., & Kumar, T. S. (2004). Anti-tumor activity and antioxidant role of *Bauhinia racemosa* against Ehrlich ascites carcinoma. *Acta Pharmacologica Sinica, 25*(8), 1070–1076.

Gupta, M., Mazumder, U. K., Kumar, R. S., Sivakumar, T., & Vamsi, M. L. (2004). Antitumor activity and antioxidant status of *Caesalpinia bonducella*. *Journal of Pharmacological Sciences, 94*, 177–184.

Gupta, M., Mazumder, U. K., Rath, N., & Mukhopadhyay, D. K. (2000**).** Antitumor activity of methanolic extract of *Cassia fistula* L. seed against Ehrlich ascites carcinoma. *Journal of Ethnopharmacology, 72*, 151–156.

Hanauske, A. R. (1993). In vitro assays for antitumor activity: More pitfalls to come? *European Journal of Cancer, 29A*(11), 1502–1503.

Izhevatkin, E. V. (2004). *Practical work on experimental oncology on example of Ehrlich ascitic carcinoma.* Nauka.

Jun-ya, U., Tezuka, Y., Banskota, A. H., Tran, Q. L., Tran, Q. K., Harimaya, Y., Saiki, I., & Kadota, S. (2002). Antiproliferative activity of Vietnamese medicinal plants. *Biological and Pharmaceutical Bulletin, 25*(6), 753–760.

Justo, G. Z., Durán, N., & Queiroz, M. L. S. (2000**).** Myelopoietic response in tumor-bearing mice by a polymer from *Aspergillus oryzae*. *European Journal of Pharmacology, 388*, 219–226.

Kasibhatla, S., & Tseng, B. (2003). Why target apoptosis in cancer treatment? *Molecular Cancer Therapeutics, 2*, 573–580.

Kavimani, S., & Manisenthil-Kumar, K. T. (2000). Effect of methanol extract of *Enicostemma littorale* on Dalton's lymphoma. *Journal of Ethnopharmacology, 71*, 349–352.

Kim, J. H., & Evans, T. S. (1964). Effects of X-irradiation on the mitotic cycle of Ehrlich ascites tumor cells. *Radiation Research, 21*, 129–143.

Kuttan, G., Vasudevan, D. M., & Kuttan, R. (1990). Effect of *Viscum album* preparation on tumour development. *Journal of Ethnopharmacology, 29*, 35–41.

Lin, Y. L., Juan, I. M., Chen, Y. L., Liang, Y. C., & Lin, J. K. (1996). Polyphenol composition in tea leaves and antiproliferative activity. *Journal of Agricultural and Food Chemistry, 44*, 1387–1394.

Loewenthal, J., & Jahn, G. (1932). Übertragungsversuche mit carcinomatöser Mäuse-Ascitesflüssigkeit. *Zeitschrift für Krebsforschung, 37*, 439–447.

Luksiene, Z., Juzenas, P., & Moan, J. (2006). Radiosensitization of tumours by porphyrins. *Cancer Letters, 235*, 40–47.

Madhuri, S., & Pandey, G. (2009**).** Some anticancer medicinal plants of foreign origin. *Current Science, 96*(6), 779–783.

Mates, J. M., Perez-Gomez, C., & De Castro, I. N. (1999). Antioxidant enzymes and human diseases. *Clinical Biochemistry, 32*(8), 595–603.

Mazumder, U. K., Gupta, M., Maiti, S., & Mukherjee, M. (1997). Antitumor activity of *Hygrophila spinosa*. *Indian Journal of Experimental Biology, 35*, 473–477.

Moongkarndi, P., Kosem, N., Luanratana, O., Kusol, S. J., & Pongpan, N. (2004). Antiproliferative activity of Thai medicinal plant extracts. *Fitoterapia, 75*, 375–377.

Muthuraman, M. S., Dorairaj, S., Rangarajan, P., & Pemaiah, B. (2008). Antitumour potential of *Tragia plukenetii*. *African Journal of Biotechnology, 7*(20), 3527–3530.

Mukherjee, A. K., Basu, S., Sarkar, N., & Ghosh, A. C. (2001). Advances in cancer therapy with plant-based natural products. *Current Medicinal Chemistry, 8*, 1467–1486.

Nagata, S. (2000). Apoptotic DNA fragmentation. *Experimental Cell Research, 256*, 12–18.

Nascimento, F. R. T., Cruz, G. V. B., Pereira, P. V. S., Maciel, M. C. G., Silva, L. A., Azevedo, A. P. S., ... & Guerra, R. N. M. (2006). Ehrlich tumour inhibition by *Chenopodium ambrosioides*. *Life Sciences, 78*, 2650–2657.

Nusse, M. (1981). Cell cycle kinetics of irradiated tumour cells. *Cytometry, 2*, 70–79.

Orrenius, S. (2004). Mitochondrial regulation of apoptosis. *Toxicology Letters, 149*, 19–23.

Ozaslan, M., Zümrütdal, M. E., Dağlıoğlu, K., Kılıç, I. H., Karagöz, I. D., Kalender, M. E., Tuzcu, M., & Çolak, O. (2009b). Antitumoural effect of *Lawsonia inermis* in mice with EAC. *International Journal of Pharmacology, 5*(4), 263–267.

Ozaslan, M., Karagöz, I. D., Kılıç, I. H., & Güldür, M. E. (2009a). Effect of *Plantago major* sap on Ehrlich ascites tumors. *African Journal of Biotechnology, 8*(6), 955–959.

Ozaslan, M., Karagöz, I. D., Kılıç, I. H., & Güldür, M. E. (2011). Ehrlich ascites carcinoma. *African Journal of Biotechnology, 10*(13), 2375–2378.

Ozaslan, M., Karagöz, I. D., Lawal, R. A., Kılıç, I. H., Çakır, A., Odesanmi, O. S., Güner, İ., & Ebuehi, O. A. T. (2016). Cytotoxic and anti-proliferative activities of *Tetrapleura tetraptera* fruit extract. *International Journal of Pharmacology, 12*, 655–662.

Pandey, G., & Madhuri, S. (2006). Medicinal plants: Better remedy for neoplasm. *Indian Drugs, 43*, 869–874.

Parkin, D. M., Freddie, M. D., Ferlay, J., & Paola, P. (2005**).** Global cancer statistics. *CA: A Cancer Journal for Clinicians, 55*, 74–108.

Paschka, A. G., Butler, R., & Young, C. Y. F. (1998). Induction of apoptosis in prostate cancer cell lines by epigallocatechin-3-gallate. *Cancer Letters, 130*, 1–7.

Patt, H. M., & Straub, R. L. (1956). Measurement and nature of ascites tumor growth. *Annals of the New York Academy of Sciences, 63*(5), 728–737.

Pezzuto, J. M. (1997). Plant-derived anticancer agents. *Biochemical Pharmacology, 53*, 121–133.

Prabhakar, B. T., Khanum, S. A., Jayashree, K., Salimath, B. P., & Shashikanth, S. (2006). Anti-tumor effects of synthetic benzophenone analogues. *Bioorganic & Medicinal Chemistry, 14*, 435–446.

Prakash, N. S., Sundaram, R., & Mitra, S. K. (2011). In vitro and in vivo anticancer activity of bacoside A from *Bacopa monnieri*. *American Journal of Pharmacology and Toxicology, 6*(1), 11–19.

Ragab, E. A., Hosny, M., Kadry, H. A., & Ammar, H. A. (2010). Acylated triterpenoidal saponins from *Gleditsia aquatica*. *Journal of Pharmacognosy and Phytotherapy, 2*(3), 24–33.

Ramakrishna, Y., Manohar, A. L., Mamata, P., & Shreekant, G. (1984). Plants and novel antitumor agents: A review. *Indian Drugs, 21*, 173–185.

Rosangkima, G., & Prasad, S. B. (2004). Antitumour activity of plants from Meghalaya and Mizoram. *Indian Journal of Experimental Biology, 42*, 981–988.

Saluja, M. S., Sangameswaran, B., Hura, I. S., Sharma, A., Gupta, S. K., & Chaturvedi, M. (2011). In-vitro cytotoxic activity of *Madhuca longifolia*. *International Journal of Drug Discovery & Herbal Research, 1*(2), 55–57.

Seraste, A., & Pulkki, K. (2000). Morphologic and biochemical hallmarks of apoptosis. *Cardiovascular Research, 45*(3), 528–537.

Sheeja, K. R., Kuttan, G., & Kuttan, R. (1997). Cytotoxic and antitumour activity of berberine. *Amala Research Bulletin, 17*, 73–76.

Shibata, M. A., Maroulakou, I. G., Jorcyk, C. L., Gold, L. G., Ward, J. M., & Green, J. E. (1996). p53-dependent apoptosis during mammary tumor progression. *Cancer Research, 56*, 2998–3003.

Smets, L. A. (1994). Programmed cell death (apoptosis) and response to anticancer drugs. *Anticancer Drugs, 5*, 3–9.

Sowemimo, A. A., Omobuwajo, O. R., & Adesanya, S. A. (2007a). Constituents of *Nymphaea lotus*. *Nigerian Journal of Natural Products and Medicine, 11*, 83–84.

Sowemimo, A. A., Fakoya, F. A., Awopetu, I., Omobuwajo, O. R., & Adesanya, S. A. (2007b). Toxicity and mutagenic activity of Nigerian plants. *Journal of Ethnopharmacology, 113*, 427–432.

Sugiura, K. (1953). Effect of various compounds on the Ehrlich ascites carcinoma. *Cancer Research, 13*, 431–441.

Sur, P., & Ganguly, D. K. (1994). Tea plant root extract as an antineoplastic agent. *Planta Medica, 60*, 106–109.

Thippeswamy, & Bharathi, P. S. (2006). *Curcuma aromatica* extract induces apoptosis and inhibits angiogenesis. *mySCIENCE, 1*(1), 79–92.

Tran, S. L., Puhar, A., Ngo-Camus, M., & Ramarao, N. (2011). Trypan blue dye enters viable cells incubated with pore-forming toxin HlyII. *PLoS ONE, 6*(9), e22876.

Walter, J. (1977). Radiation hazards and protection. In *Cancer and radiotherapy*. Churchill: Livingstone.

Wolfe, N. (1986). Neoplasia. In *Cell, tissue and disease: The basis of pathology*. Baillière Tindall.

Wyllie, A. H. (1980). Glucocorticoid-induced thymocyte apoptosis. *Nature, 284*, 555–556.

Yarbro, C., Frogge, M., & Goodman, M. (2005). *Cancer nursing: Principles and practice* (6th ed.). Jones & Bartlett Learning.

Zimmerman, K. C., Bonzon, C., & Green, D. (2001). The machinery of cell death. *Pharmacology & Therapeutics, 92*, 57–70.

Zumrutdal, M. E., Ozaslan, M., Tuzcu, M., Kalender, M. E., Dağlıoğlu, K., & Akova, A. (2008). Effect of *Lawsonia inermis* on mice with sarcoma. *African Journal of Biotechnology, 7*(16), 2781–2786.

Zhong, L., Qu, G., Li, P., Han, J., & Guo, D. (2003). Induction of apoptosis by gleditsioside E. *Planta Medica, 69*, 561–563

Author(s) Information

Ridwan Lawal
University of Lagos,
Lagos, Nigeria
Contact e-mail: *alawal@unilag.edu.ng*

Mehmet Ozaslan
Gaziantep Universitesi
Gaziantep, Türkiye

Dayo Adedoyin
Yaba College of Technology
Yaba, Lagos, Nigeria

Obumneme P. Okoye
University of Lagos,
Lagos, Nigeria

To cite this article:

Lawal, R., Ozaslan, M., Adedoyin, D., & Okoye O.P. (2025). Cytotoxic and antiproliferative activities of Nymphaea lotus and 5-fluorouracil on Ehrlich ascites carcinoma cells. *The Eurasia Proceedings of Health, Environment and Life Sciences (EPHELS), 20,* 19-31.

The Eurasia Proceedings of Health, Environment and Life Sciences (EPHELS)
ISSN: 2791-8033

The Eurasia Proceedings of Health, Environment and Life Sciences (EPHELS), 2025

Volume 20, Pages 32-44

ICMeHeS 2025: International Conference on Medical and Health Sciences

Screening of Bioactive Secondary Metabolites of *Streptomyces spp.* Isolated from the Sediments

Khansa M. Younis
University of Mosul

Abstract: The purpose of this study was to assess the activity of Streptomyces spp., isolate and identify them from samples of silt soil and Tigris river water in Mosul, Iraq. Variations in the isolates' microscopic and biochemical properties were used to identify them., such as soluble pigment, aerobic mycelium, and substrate mycelium. Using the perpendicular streak method, eight of the twelve actinomycete isolates that were isolated from the water and sediments of the Tigris River exhibited antibacterial activity against specific pathogenic bacteria. *Staphyloccocus aureus* (MTCC 3260), *Vibrio parahaemolyticus*, *Klibsiella pneumoniae, Salmonella typhi, Proteus mirabilis, E. coli* (MTCC 443), *Pseudomonas aeruginosa (MTCC 424), and Aeromonas hydrophila bacteria were all susceptible to the broad-spectrum activity of isolate Sediment Lake Iraq E2.* According to the findings of phylogenetic analysis, isolate E2 shared the closest kinship with Streptomyces sp. (EU257231). Using high-performance liquid chromatography (HPLC), the Streptomyces isolate E2's secondary metabolite was further examined. There is evidence that these secondary metabolites are harmless and may have antibacterial properties against human pathogens.

Keywords: Tigris river, Secondary metabolites, Antimicrobial, *Streptomyces*.

Introduction

Marine environment is largely untapped source for the isolation of new microorganisms with potentiality to produce active secondary metabolites. Among such microorganisms, actinomycetes are of special interest, since they are known to produce chemically diverse compounds with a wide range of biological activities (Bredholt et al., 2008).

Actinomycetes are filamentous bacteria that produce antibiotics. It has long been recognized that Streptomyces species exhibit two distinct growth phases, referred to as the primary and secondary mycelium, respectively. These phases are the substratum mycelium and the aerial mycelium, they are found in freshwater and marine water habitats (Fenical & Jensen, 2006; Weinstein et al., 2005). The dominant actinomycetes Micromonospora can be isolated from aquatic habitats such as streams, rivers, lake mud, river sediments, beach sands, sponge and marine sediments (Rifaat, 2003; Eccleston et al., 2008).

A multitude of novel bioactive compounds have been identified from aquatic actinomycetes, such as rifamycin originating from Micromonospora (Huang et al., 2008), salinosporamide-A, an anticancer metabolite derived from a Salinispora strain (Fehling et al., 2003), marinomycins sourced from Marinophilus sp. (Jensen et al., 2005); abyssomicin-c extracted from Verrucosispora sp. and Marino pyrroles obtained from Streptomyces sp. (Riedlinger et al., 2004; Hughes et al., 2008).

Out of a total of 22,500 biologically active compounds derived from microbial sources, 45% are attributed to actinomycetes, 38% to fungi, and 17% to other bacterial taxa (Berdy, 2005; Hayakawa et al., 2007). The genus

Streptomyces is responsible for over 70% of the overall antibiotic production, while Micromonospora represents less than one-tenth of the quantity produced by Streptomyces (Lam, 2006; Gurung, et al.,2009).

Valli et al. (2012) meticulously conducted a comprehensive investigation wherein they successfully isolated a total of 21 potential actinomycetes derived from a diverse range of marine environmental samples, and subsequently documented that each and every one of the isolates exhibited promising antimicrobial activity against at least one of the tested pathogenic organisms, as reported in their pivotal study (Vali, et al., 2012). In a similar vein, Kalyani et al. (2012) undertook an extensive isolation process that yielded 20 distinct species from marine soil samples, among which three species demonstrated a significant level of antimicrobial efficacy against the notorious pathogens S. aureus and E. coli, thus contributing valuable insights to the field of microbiological research (Kalyani, et al., 2012).

Multiple drug-resistant pathogenic strains caused significant morbidity and mortality, particularly among elderly and immunocompromised patients. Antimicrobial drugs used for prophylactic or therapeutic purposes in human, veterinary, and agricultural settings were favoring the survival and spread of resistant organisms (Barsby et al., 2001; Parungao et al., 2007). The goal is to improve or discover a new class of active compounds that function differently from antibiotics in order to solve this problem. It was essential to continually screen secondary microbial products derived from potential bacterial taxa in order to identify novel chemicals for the development of new medical treatments (Lazzarini et al., 2000). Many researchers are now looking for novel antibiotics in many unexplored ecosystems to determine whether they produce antibiotics (Oskay et al., 2004). Consequently, the purpose of this work was to evaluate the activities of Streptomyces spp. And extract and identify them from samples of Tigris River water and sediments in Mosul, Iraq.

Method

Sampling Area

The samples of water and sediments were collected from Tigris river in Mosul, Iraq.

Sample Collection

Totally 10 water and 10 sediment samples were collected. The water samples were collected. İn 500 ml sterile screw capped bottles and sufficient space was provided for aeration and thorough mixing. The sediments were collected by sterilized spatula transferred to wide mouth sterilized bottle. All samples were labeled and transported to the Microbiology Laboratory/ College of science/University of Mosul.

Isolation and Identification Streptomyces spp.

Actinomycetes agar served as the medium for the marine actinomycetes' isolation and culture. After autoclaving, 50 and 20 μg mL^{-1} of tetracycline and nystatin, respectively, were added to the medium as antibacterial and antifungal agents to prevent bacterial and fungal contamination. One gram of dried Tigris river silt soil samples was combined with 99 milliliters of sterile distilled water to make the stock suspension. Then, for 30 minutes at room temperature, the materials were agitated in a shaker that was set to 120 rpm. After being serially diluted from 10^{-1} to 10^{-3}, the stock suspension was let to sit for ten minutes. 0.1 ml of each dilution—water and sediments—was pipetted and put on actinomyces agar after shaking.

The suspension was thereafter uniformly applied throughout the media's surface with a sterile brush. The inoculation plates were cultured at 28°C for 7 to 14 days, and chosen isolates were aseptically streaked on actinomyces and nutritional agar, followed by incubation at 28°C for 7 days. Pure culture was inoculated onto slants and stored at 4°C for further analysis. Morphological traits, including colony features, pigment synthesis, and the presence or absence of aerial and substrate mycelium were examined (Oskay et al., 2004).

Morphological and Physiological Characterization

Following inoculation on specific medium (SCA, MA, NA, PDA, and ISP2), the obtained actinomycete isolates were grown for seven days at 30°C and observed daily. Actinomycete isolates were analyzed for

micromorphology, including gram staining, morphology, and dimensions under a light microscope, alongside culture characteristics such as colony morphology, comprising surface elevation, texture, density, coloration of aerial and substrate mycelium, and pigment synthesis.

Biochemical Characterization

The Streptomyces isolates were characterized by conventional biochemical tests. The tests encompass the following: cytochrome oxidase, catalase, tween-40, tween-60, tween-80, esculin, glucose gas production, casein hydrolysis, urea hydrolysis, nitrate reduction, hydrogen sulfide production, methyl red test, indole test, Voges-Proskauer test, citrate utilization test, and glucose gas production. The isolates were inoculated in actinomycetes broth enriched with specific sugars and incubated for seven days at 28°C to evaluate acid production from various carbohydrate sources, including adonitol, fructose, sorbitol, dextrose, lactose, inositol, maltose, sucrose, raffinose, and xylose.

Select Bacteria for Antibacterial Activity

The selected human microbiological pathogens for the assessment of antibacterial activity included *Staphylococcus aureus* (MTCC 3260), *Vibrio parahaemolyticus, Klebsiella pneumoniae, Salmonella typhi, Proteus mirabilis, Escherichia coli* (MTCC 443), *Pseudomonas aeruginosa* (MTCC 424), and *Aeromonas hydrophila*. The bacteria were obtained from the Microbiology Laboratory at the College of Science and were activated by culture in Nutrient Broth at 37°C for 24 hours.

Primary Screening (Cross Plate Technique)

Streptomyces isolates were inoculated into nutrient agar plates by streaking the middle of each plate. The examined bacterial pathogens were inoculated perpendicularly to the Streptomyces (a single streak at a 90° angle to the Streptomyces isolates) once the Streptomyces had fully developed after 7 days of incubation at 28ºC. The plates were subsequently re-incubated at 37°C following a 24-hour period. When the reference strains did not proliferate near the Streptomyces line, the antibacterial action was observable to the naked eye.

Secondary Evaluation (Antagonistic Activity)

The most active Streptomyces isolates were cultured in 250 mL flasks using 50 mL of actinomycetes broth. Following seven days of incubation at 28°C, the cultures underwent centrifugation for fifteen minutes at 10,000 rpm. The antibacterial activity of the clear supernatant broth was assessed against a range of human pathogenic pathogens using the agar well diffusion method. Fifty microliters of crude culture supernatant was dispensed into each well, and following a 24-hour incubation of the bacterial species at 37 °C, the diameters of the inhibitory zones were measured. The most potent active streptomyces isolate was chosen for the next testing.

Extraction of Streptomyces Isolates Secondary Metabolites

The cultivation conditions, incubation duration, and fermentation medium were refined for the identification of secondary metabolite chemicals. These include cultivating Streptomyces isolates in 1 liter of ISP2 medium (comprising 3 g of yeast extract, 3 g of malt extract, 10 g of glucose, and supplemented with 0.5 ml of glycerol) in 2-liter flasks, incubated for 9 days at 29°C with shaking at 200 rpm. An adapted approach from Jensen et al. (2007). The bioactive metabolite compounds were isolated by an extraction procedure. The bacterial culture of each isolate was centrifuged for 15 minutes at 10,000 rpm, after which the cell-free supernatant was collected, mixed with an equivalent volume of ethyl acetate, and incubated on a rotary shaker at 200 rpm overnight. The solvent layer was collected and subsequently evaporated using a rotary evaporator to get the crude extracts. Pure dimethyl sulfoxide (DMSO) was subsequently included into the crude extract to formulate a 50 mg/mL (w/v) stock, which was then preserved at 4 °C for use in the agar diffusion experiment.

Agar Diffusion Assay

Cultured overnight twenty milliliters of nourishing broth medium were inoculated with 500 microliters of the selected human pathogenic bacteria, followed by incubation for two to three hours at 30°C. An optical density of 0.7 at 600 nm was achieved by shaking at 170 rpm. The agar overlay test employed semi-solid nutritional agar (0.8% agar), maintained at 45°C. Ten milliliters of culture (OD 600nm = 0.7) were included before plating the supernatants onto the medium. Wells in the plate were created with a sterile cork borer with a diameter of 6 mm. Each well was then filled with 30 µL of streptomyces supernatants. Antibacterial activity was detected in a zone of clearing at the center. The fresh nutrient broth served as the negative control. Three duplicates of the bioassay were performed, and the mean value was applied. The following tests were conducted using the isolate that was the most active.

DNA Extraction

The bead beater-phenol extraction method was used to prepare the DNAs (Ko et al., 2002). A 2.0 ml screw-cap microcentrifuge tube was filled with 100 ml (packed volume) of glass beads (diameter, 0.1 mm; Biospec Products, Bartlesville, Okla., U.S.A.) and 100 ml of phenol-chloroform-isopropyl alcohol (50:49:1), and a loopful of each isolate's culture was suspended in 200 ml of TEN buffer (10 mM Tris-HCl, 1 mM EDTA, 100 mM NaCl; pH 8.0). After one minute of oscillating the tube on a Mini-Bead Beater (Biospec Products) to disturb the bacteria, the phases were separated by centrifugation (12,000 ×g, 5 min). Following the transfer of the aqueous phase to a different tube, 250 ml of ice-cold ethanol and 10 ml of 3 M sodium acetate were added. The mixture was then maintained at 20 °C for 10 minutes in order to precipitate the DNA.Thereafter, the DNA pellet was washed with 70% ethanol, dissolved in 60 ml of TE buffer (10 mM Tris-HCl, 1 mM EDTA; pH 8.0), and used as the template for PCR.

Polymerase Chain Reaction (PCR) Amplification of the 16S rRNA Gene

The 16S rRNA gene was sequenced to identify the selected streptomyces isolate. PCR products obtained from the total genomic DNA were used to amplify the 16S rRNA using the forward primer and reverse primer 8F: (5’ AGA GTT TGA TCC TGG CTC AG 3’) 1492R: (5’ ACG GCT ACC TTG TTA CGA CTT 3’) (Deepa et al., 2013).

PCR was performed in a 50 L reaction mixture that contained 10 □L of 5X GoTaq Flexi buffer, 1□L of 0.2 mM PCR–grade of deoxynucleoside triphosphate (dNTP), 8□L of 4mM MgCL2, 1□L of 1□M reverse primer, 1□L of 1□M forward primer, 1□Lof 0.5□g DNA template, 0.25□L of 1.25 u Go Taq DNA polymerase, and 27.75 L of sterile Milli–Q water. A Bio–Rad MyCycler thermal cycler (Bio–Rad, USA) was used to carry out PCR at an initial denaturation step with 95oC temperature for 2 min, 35 cycles of 95oC for 1 min, at 50oC for 1 min, at 72oC for 1 min, and a final extension step at 72oC for 5 min. The amplification DNA products were separated by electrophoresis technique on 1.5 % (w/v) agarose gel in 1X TAE buffer (40 mMTris acetate, 1 mM EDTA, pH 8.0) at 80 V for 45 min, following PCR amplification. The gel was pre-stained with FloroSafe DNA stain while 1 kb DNA ladder was used as DNA size marker. Finally, all gels were viewed and captured by UV trans illuminator Gel Documentation System (Syngene, UK). A comparison between the sequences available online and the obtained DNA sequences was done using the gen bank database (http://www.ncbi.nlm.nih.gov). utilizing the online bioinformatics resources, such as BLAST (www.ncbi.nlm.nih.gov/BLAST). A phylogenetic tree comprising a chosen isolate and additional related genera that are available in the NCBI database was created using a homology search using Clustal X 1.8. The evolutionary history was inferred using MEGA6's neighbor-joining approach. 1000 bootstrap replicates of the original sequence data were used to assess each branch's confidence value.

High Performance Liquid Chromatography (HPLC) Chromatography

Separation of the bioactive components from the secondary metabolites of the active isolate was performed using HPLC on a C_{18}, 3µm column with acetonitrile: methanol: propanol (40:50:10). The flow rate was 0.8 ml/min.

Results and Discussion

The physical characteristics of the identified Streptomyces isolates are displayed in figure (1). The suspected colonies were cultivated on agar and chosen based on their morphology (they had a smooth surface initially, but as the aerial mycelium formed, they became soft, granular, and powdery) and color (either gray, creamy, or white), with colony diameter sizes ranging from 1 to 10 mm. The identification, characterization, and classification of Actinomycetes rely on many features that should stay constant when the microbe is isolated under similar growth conditions (Reddy et al., 2011). Actinomycetes sourced from marine environments are well-documented to thrive on starch casein agar (SCA) (Laidi et al., 2006; Hemashenpagam, 2011; Reddy et al., 2011). Consequently, SCA augmented with 50% old natural seawater, aged for 30 days, was employed to extract streptomycete strains, which were noted to flourish abundantly on this medium, the colony morphologies and the surface and aerial mycelium, as delineated in this study, are characteristic of Streptomycetes spp. Colony morphology has often been employed to identify Actinomycetes (Oskay et al., 2004; Hemashenpagam, 2011; Reddy et al., 2011)

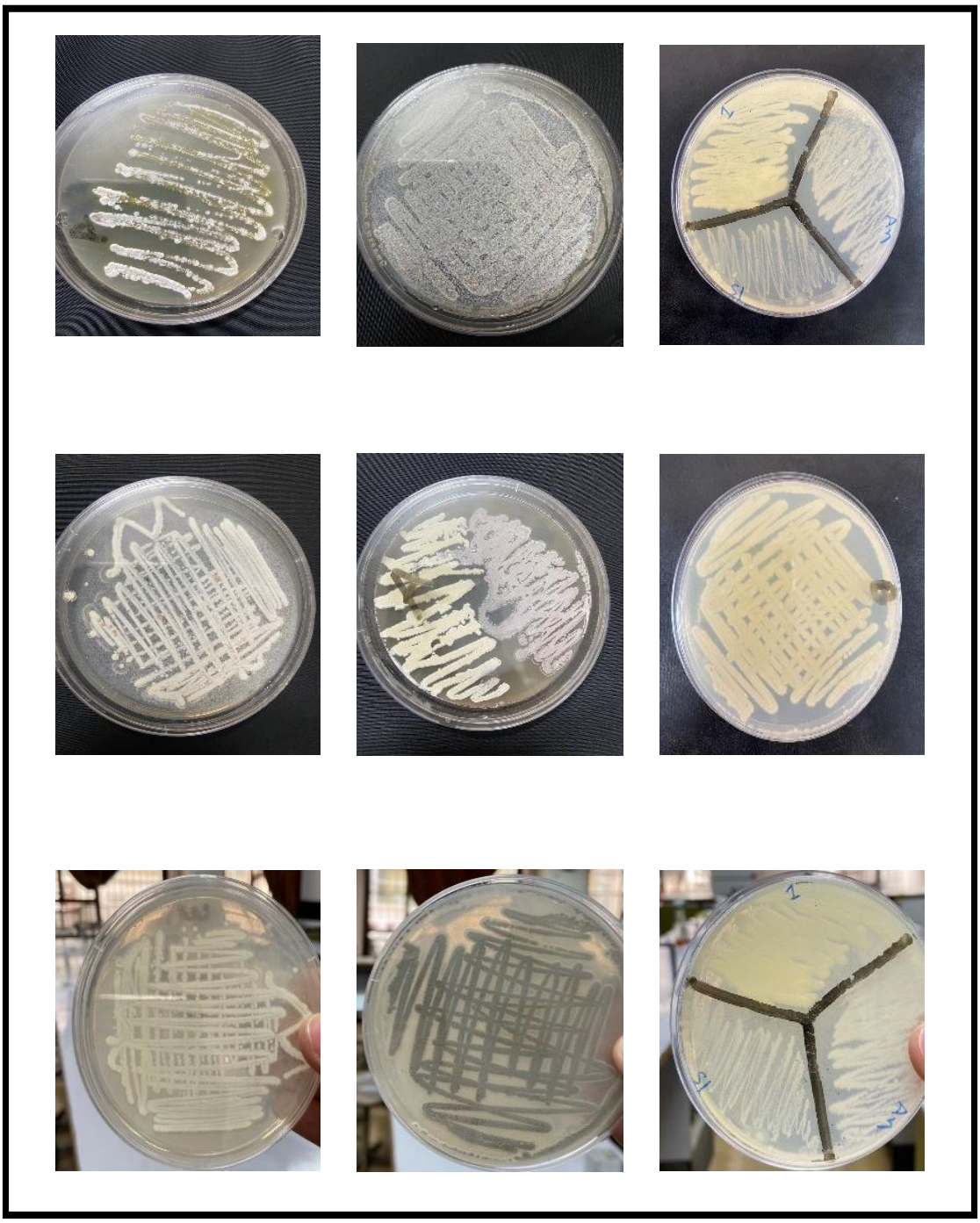

Figure 1. Arial mycelium of streptomyces isolates grown on actenimycetes agar.

The isolates were examined under microscope after 7-14 days of incubation to see the Gram positive bacteria hyphae as shown in Figure 2.

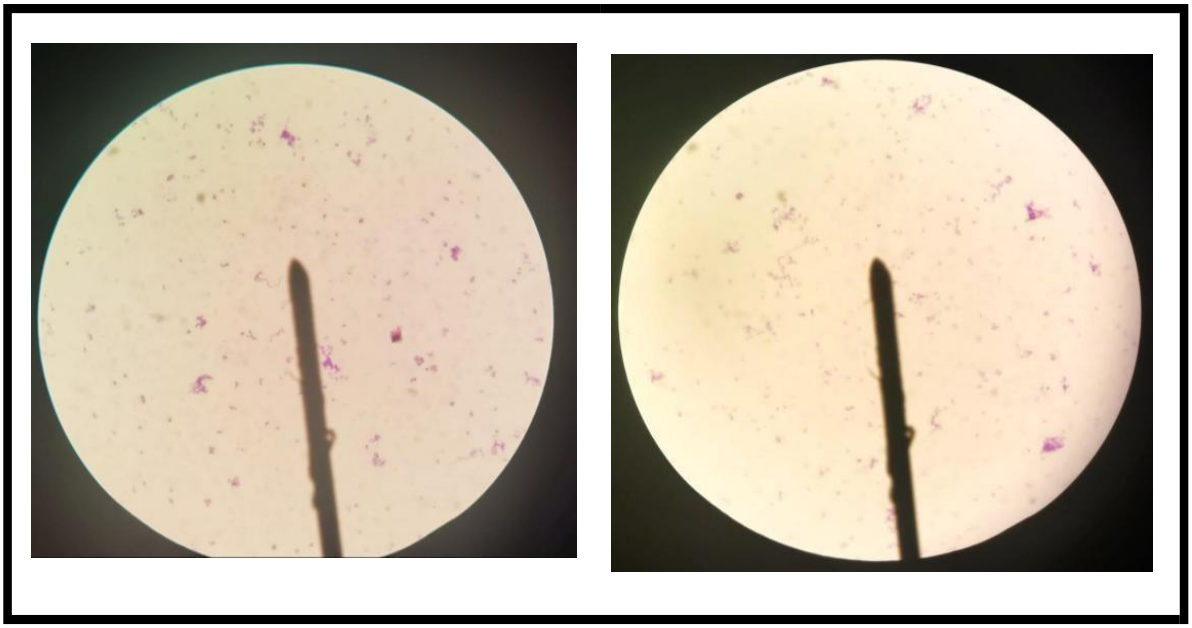

Figure 2. Microscopic examination: Gram positive bacteria, forming hyphae

Twelve isolate designated E1-E12, showed varied morphological characteristics (Table 1). The growth and colony morphology of streptomyces isolates were observed to grow very well on all the 6 selected media (SCA, MA, NA, PDA, ISP2 and Actinomycetes agar). Diffusible pigment on the other hand was absent in all the media. Chemotaxonomy is the examination of chemical variations among species and the application of chemical characteristics for classification and identification. This is one of the effective methods for identifying the genera of actinomycetes (Remya &Vijayakumar, 2008).

The actinomycetes isolated in this investigation were identified as Streptomyces based on their morphological, physiological, pigment production and biochemical characteristics (Suneetha et al., 2011; Bundale et al., 2015; Singh et al., 2016). Their compact, chalk-like, dry colonies, which ranged in hue from pink to white, demonstrated strong sporulation. According to Suneetha et al. (2011), the isolates were determined to be gram-positive organisms with branching mycelium in their cell shape. Gelatin, casein, and starch were all hydrolyzed effectively by the isolates (Manteca &Sanchez, 2009). Catalase was positive in every isolation, although indole synthesis was completely negative.

Table 1. Morphological characterization of streptomyces isolates

Media types	Growth	Aerial mycelium	Substrate mycelium	Diffusible pigment
SCA	+++	White	Beige	Absent
MA	+++	White	Beige	Absent
NA	+++	White	Beige	Absent
PDA	+++	Grey	Brown	Absent
ISP 2	+++	White	Pale yellow	Absent
Actinomycetes agar	+++	White Grey	Beige	Absent

Physiological and Biochemical Characteristics of Streptomyces Isolates

Streptomycete isolates' physiological and biochemical traits were displayed in Table 2. Oxidase, starch agar, urea hydrolysis, skim milk agar, mannitol, xylose, D-galactose, D-Fructose, L- Arabinose, and citrate utilization were all detected in the long filamentous, Gram-positive isolates. Additionally, the isolates tested negative for non-motile, Rhamnose VP gelatin hydrolysis, and xanthine agar

Table 2. Physiological and biochemical characteristics of the Streptomyces isolates

Characteristics	Streptomycetes spp
Gram stain	Positive
Shape and growth	Long filamentous
Motility	Non-motile
Starch hydrolysis	+
Oxidase	+
Casein hydrolysis	+
Urea hydrolysis	+
Gelatin Hydrolysis	+
Skim milk agar	+
Xanthine Agar	-
Mannitol	+
Indole	-
Catalase	+
Xylose	+
Rhamnose	-
D-Galactose	+
D-Fructose	+
L-Arabinose	+
Citrate utilisation	+
VP	-
TSI	Alk/Alk

Primary Screening of Isolates

During the primary screening, isolates were screened against selected pathogenic bacteria strains by using perpendicular streak. The zone of inhibition near the colonies were observed, (Figure 3)

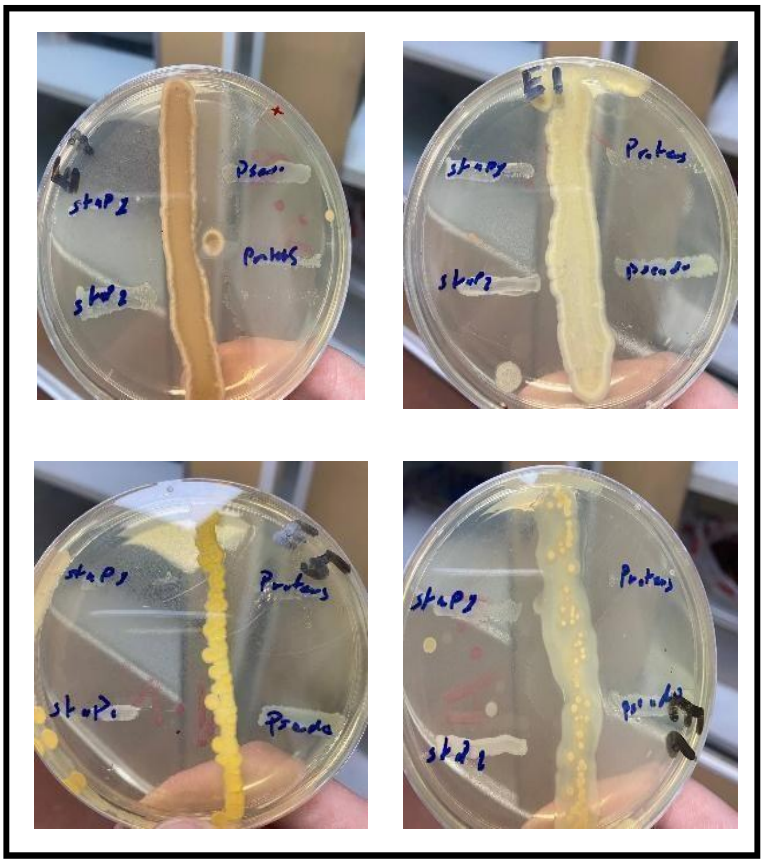

Figure 3. Antimicrobial activity of *Streptomyces* isolates against selected pathogenic bacteria using perpendicular streak.

Among the 12 streptomyces isolate from water sediments of Tigris river, 8 isolates showed antibacterial activities against at least bacteria, therefor were chosen for the following experiments.

Antibacterial Activities of *Streptomyces* Secondary Metabolites

Figure 4 displays the E2 isolate's antibacterial properties against a subset of human pathogenic microorganisms. When tested against the chosen bacterium, the isolate showed varied levels of antibiotic activity. (A. hydrophilia, S. aureus, K. pneumoniae, E. coli, P. aerogenosa, S. typhi, and V. parahaemolytica).The results showed themaximum activity against *V. parahaemolyticus, S. aureus, A. hydrophilia* and *S. typhi* while the least activity was found against *E. coli*.

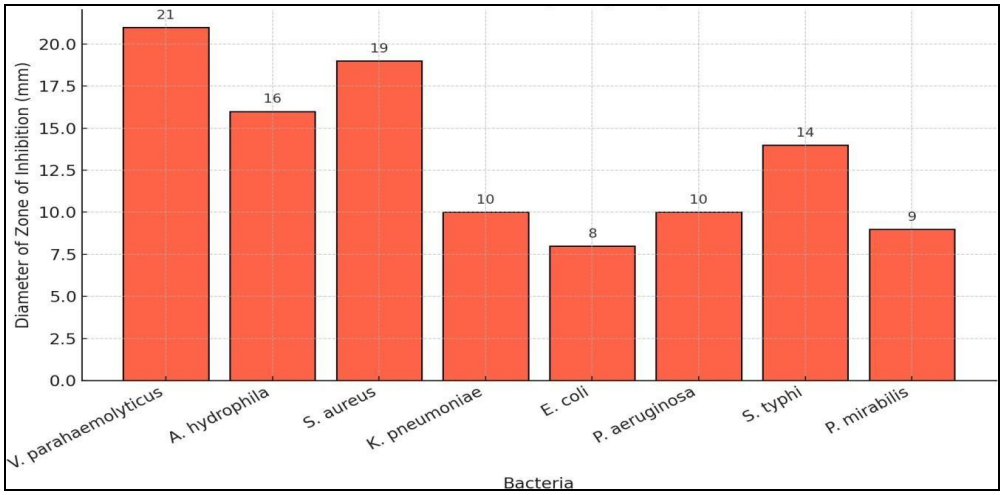

Figure 4. Antibacterial activities of *Streptomyces* strain E2 against selected pathogenic bacteria

Diverse microorganisms possess distinct needs for culture conditions and optimal parameters for antibiotic manufacture; these elements affect bacterial development, subsequently influencing antibiotic synthesis (Yoshida et al., 1972; Akhurst, 1982; Geetha & Vinoth, 2012). Actinomycetes are recognized for their ability to produce antibiotics (Geetha & Vinoth, 2012). Among the genera of actinomycetes, Streptomyces is a notably prolific source of natural products, generating two-thirds of commercially available antibiotics (Bentley et al., 2002). The selected E2 isolate in this study exhibited significant antagonistic activity against seven human pathogenic pathogens, with the most pronounced effect shown against S. aureus and V. parahaemolyticus. These findings align with those seen in prior pertinent studies (Remya & Vijayakumar, 2008; Geetha and Vinoth, 2012; Singh et al., 2014; Singh et al., 2016)

PCR and Gel Electrophoresis

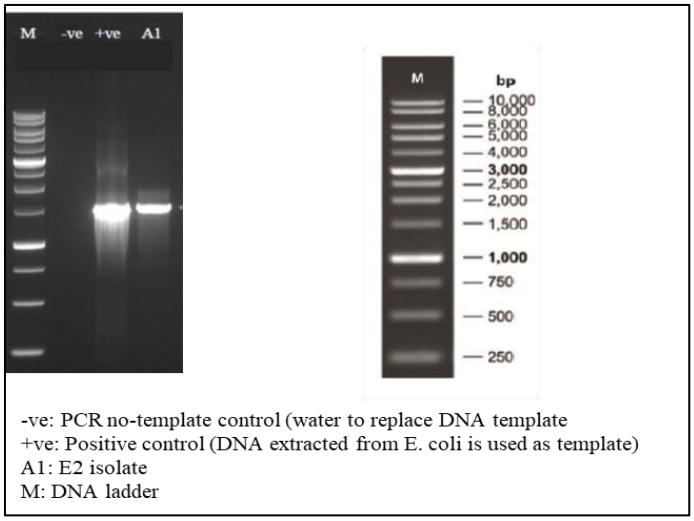

Figure 5. Gel electrophoresis of PCR products from *Streptomyces* strain E2

The PCR products obtained following the protocol earlier described were subjected to gel electrophoresis and the result is photographed as shown in Figure 5.

Phylogenetic Analysis

Based on a small portion of the 1500 bp rRNA gene, neighbor-joining phylogenetic trees were calculated using the Kimura 2-parameter approach to show the evolutionary relationship between Streptomyces found in this study and those curated in genbank (Kimura, 1980). After gaps and unclear residues were eliminated, 1138 nucleotide locations in total were examined. To increase clade confidence, 1,000 bootstrap repeats were carried out (Felsenstein, 1985). Streptomyces species retrieved from the NCBI Genbank are marked with their accession numbers, while those isolated from our sample in this study are denoted with a red triangle. The study's phylogenetic tree demonstrates the tight relationship between the Streptomyces collected for this investigation and those curated in the Genbank (Figure 6).

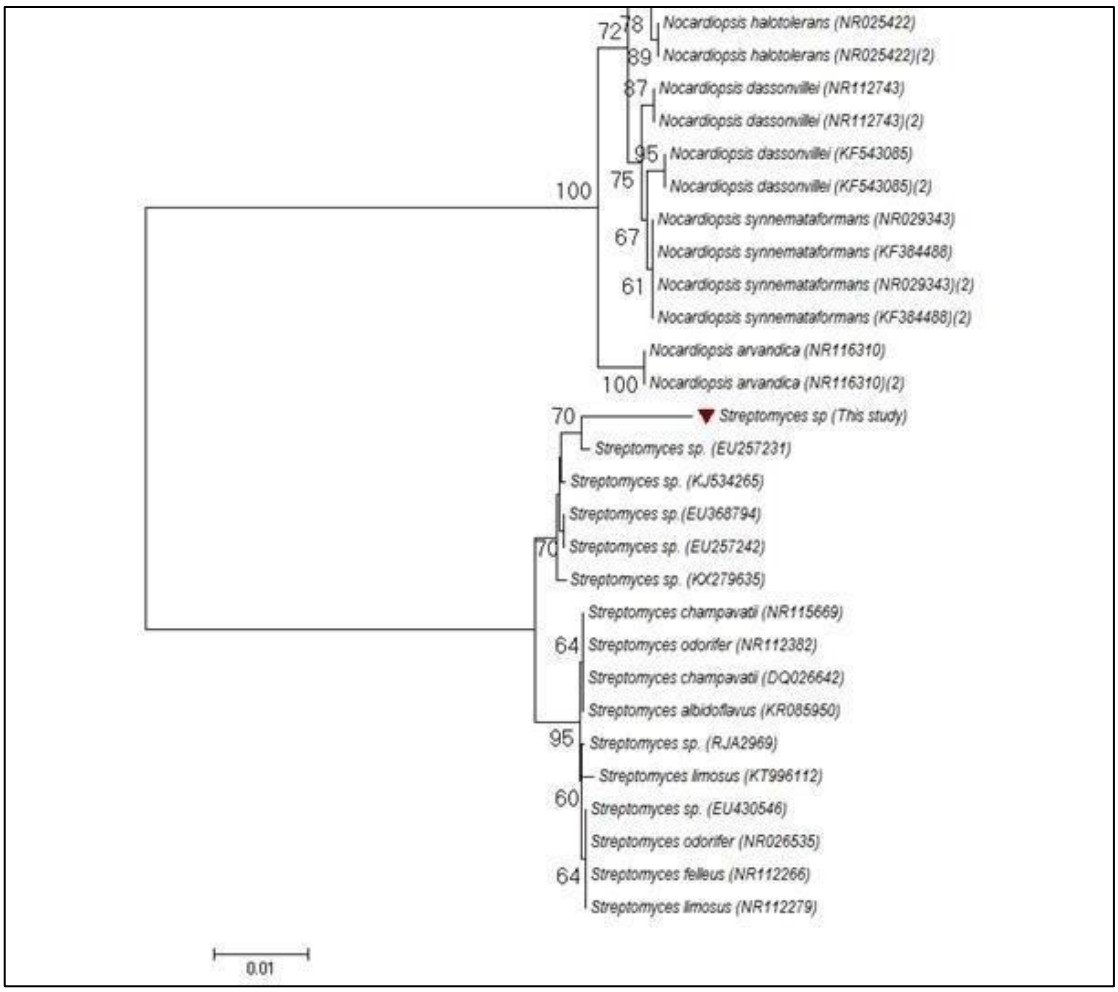

Figure 6. Neighbor-Joining phylogenetic assessment.

The tree is shown to scale, with branch lengths corresponding to the same units as the evolutionary distances employed to deduce the phylogenetic tree. The evolutionary distances were calculated using the Kimura 2-parameter approach, expressed in terms of base substitutions per site. The study encompassed 36 nucleotide sequences. All entries with gaps and absent data were removed. Evolutionary studies were performed using MEGA6.

The phylogenetic analysis of 16SrDNA genes in streptomycetes, conducted through DNA extraction and amplification of the gene encoding 16SrDNA via Polymerase Chain Reaction, has emerged as a widely adopted technique for the identification of streptomycete isolates (Vijayakumar et al., 2005; Abdelmohsen et al., 2010; Deepa et al., 2013). This work utilized Neighbour-joining phylogenetic analysis using the Kimura 2-parameter approach to clarify the evolutionary connections of the selected streptomyces isolate, based on a small segment

of roughly 1500 bp of the rRNA gene. The findings revealed that the selected E2 isolate is tightly associated with Streptomyces and Nocardia species, respectively.

High Performance Liquid Chromatography

The chemical composition of bioactive extract of Streptomyces strain E2 was investigated using HPLC analysis (Maleki & Mashinchian, 2011; Kumar et al., 2014). And the result is shown in Figure 7. Twenty two peaks were observed following the analysis. The study's findings indicate that the E2 isolate has active compounds that absorb most efficiently throughout the range of 380 to 450 nm. According to comparable studies (Ezra et al., 2004; Kumar et al., 2009), the majority of peptide antibiotics exhibit peak absorbance in the ranges of 210 to 230 nm and 270 to 280 nm. The antibiotic activities demonstrated by the isolate may result from these peptide antibiotics.

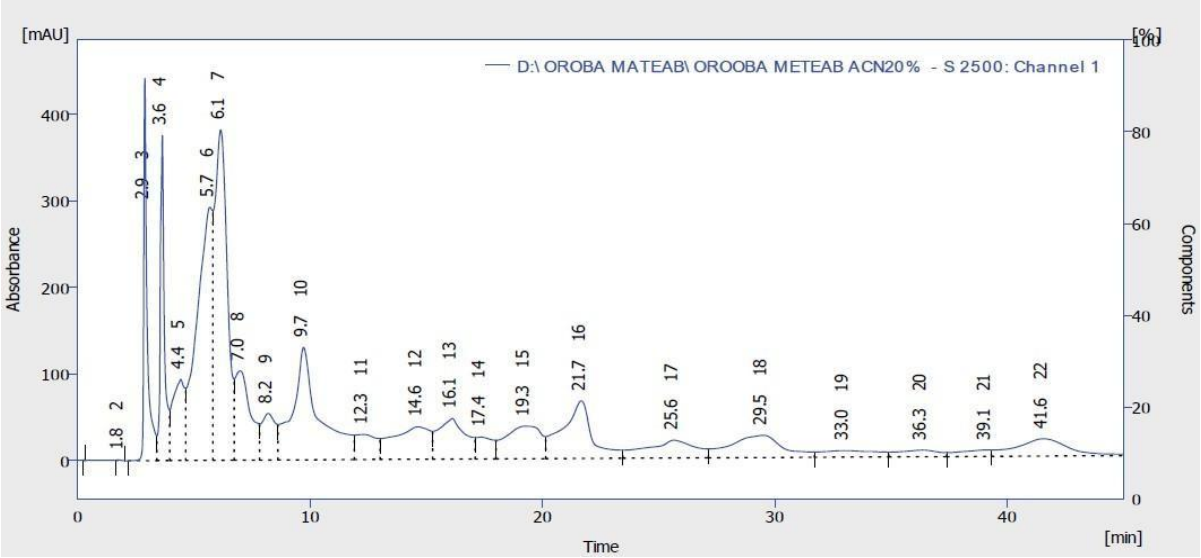

Figure 7. Analysis HPLC chromatogram of Streptomyces strain E2 secondary metabolites

Conclusions

Based on the findings of this study, the sediments of the Tigris river in Mosul/Iraq is a fertile land of isolation Streptomycetes which have varying cultural, morphological, biochemical and carbon source requirements. Some of the actinomycetes could be having antibiotics of medical important thus there is need to further screen the isolates for antibiotics production. The streptomycete isolates obtained could be subjected to further analysis for the production of potent antibiotics that could mitigate the issues of antibiotic resistance. The confirmation of novelty of these compounds need further investigations in order to determine the functional groups, clarify the structure and physicochemical nature of the antibiotics

Scientific Ethics Declaration

* The author declares that the scientific ethical and legal responsibility of this article published in EPHELS journal belongs to the author.

Conflicts of Interest

* The author declares no conflict of interest.

Funding

* This research received no specific grant from any funding agency in the public, commercial, or not-for-profit sectors.

Acknowledgements or Notes

* This article was presented as a poster presentation at the International Conference on Medical and Health Sciences (www.icmehes.net) held in Antalya/Türkiye on November 12-15, 2025.

Reference

Abdelmohsen, U. R., Pimentel-Elardo, S. M., Hanora, A., Radwan, M., Abou-El-Ela, S. H., Ahmed, S., & Hentschel, U. (2010). Isolation, phylogenetic analysis and anti-infective activity screening of marine sponge-associated actinomycetes. *Marine Drugs, 8*(3), 399–412.

Akhurst, R. J. (1982). Antibiotic activity of *Xenorhabdus* spp., bacteria symbiotically associated with insect pathogenic nematodes of the families Heterorhabditidae and Steinernematidae. *Journal of General Microbiology, 128*, 3061–3065.

Barsby, T., Kelly, M. T., Gagné, S. M., Andersen, R. J., & Bogorol, A. (2001). A cationic peptide antibiotic produced in culture by a marine *Bacillus* sp.: A novel template for peptide antibiotics. *Organic Letters, 3*, 437–440.

Bentley, S. D., Chater, K. F., Cerdáno-Tarraga, A. M., …& Challis, G. L. (2002). Complete genome sequence of the model actinomycete *Streptomyces coelicolor* A3(2). *Nature, 417*, 141–147.

Berdy, J. (2005). Bioactive microbial metabolites: A personal view. *Journal of Antibiotics, 58*(1), 1–26.

Bredholt, H., Fjærvik, E., Jhonsen, G., & Zotchev, S. B. (2008). Actinomycetes from sediments in the Trondheim Fjord, Norway: Diversity and biological activity. *Marine Drugs, 6*, 12–24.

Bush, K., & Macielag, M. (2000). New approaches in the treatment of bacterial infections. *Current Opinion in Chemical Biology, 4*, 433–439.

Cwala, Z., Igbinosa, E. O., & Okoh, A. I. (2011). Assessment of antibiotics production potential in four actinomycetes isolated from aquatic environments of the Eastern Cape Province of South Africa. *African Journal of Pharmacy and Pharmacology, 5*(2), 118–124.

Deepa, S., Kanimozhi, K., & Panneerselvam, A. (2013). 16S rDNA phylogenetic analysis of actinomycetes isolated from marine environment associated with antimicrobial activities. *Hygeia Journal for Drugs and Medicines, 5*(2), 43–50.

Dharmaraj, S., Ashokkumar, B., & Dhevendaran, K. (2009). Fermentative production of carotenoids from marine actinomycetes. *Iranian Journal of Microbiology, 1*(4), 133–138.

Eccleston, G. P., Brooks, P. R., & Kurtböke, D. I. (2008). The occurrence of bioactive micromonosporae in aquatic habitats of the Sunshine Coast in Australia. *Marine Drugs, 6*, 243–261.

Ellaiah, P., Kalyan, D., Rao, V. S., & Rao, B. V. (1996). Isolation and characterization of bioactive actinomycetes from marine sediments. *Hindustan Antibiotics Bulletin, 38*, 48–52.

Enright, M. C. (2003). The evolution of a resistant pathogen: The case of MRSA. *Current Opinion in Pharmacology, 3*, 474–479.

Ezra, D., Castillo, U. F., Strobel, G. A., Hess, W. M., Porter, H., Jensen, J. B., …& Hunter, M. (2004). Coronamycins, peptide antibiotics produced by a verticillate *Streptomyces* sp. (MSU-2110) endophytic on *Monstera* sp. *Microbiology, 150*(4), 785–793.

Fehling, R. H., Buchanan, G. O., Mincer, T. J., Kauffman, C. A., Jensen, P. R., & Fenical, W. (2008). A highly cytotoxic proteasome inhibitor from a novel microbial source, a marine bacterium of the new genus *Salinospora*. *Angewandte Chemie International Edition, 42*, 355–357.

Felsenstein, J. (1985). Confidence limits on phylogenies: An approach using the bootstrap. *Evolution, 39*, 783–791.

Fenical, W., & Jensen, P. R. (2006). Developing a new resource for drug discovery: Marine actinomycete bacteria. *Nature Chemical Biology, 2*, 666–673.

Gold, H. S., & Moellering, R. C. (1996). Antimicrobial-drug resistance. *New England Journal of Medicine, 335*, 1445–1453.

Gurung, T. D., Sherpa, C., Agrawal, V. P., & Lekhak, B. (2009). Isolation and characterization of antibacterial actinomycetes from soil samples of Kapa Pathar, Mount Everest Region. *Nepal Journal of Science and Technology, 10*, 173–182.

Hayakawa, Y., Shirasaki, S., Shiba, S., Kawasaki, T., Matsuo, Y., & Adachi, K. (2007). Piericidins C7 and C8: New cytotoxic antibiotics produced by a marine *Streptomyces* sp. *Journal of Antibiotics, 60*, 196–200.

Hemashenpagam, N. (2011). Purification of secondary metabolites from soil actinomycetes. *International Journal of Microbiology Research, 3*(3), 148–156.

Hu, H., & Ochi, K. (2001). Novel approach for improving the productivity of antibiotic-producing strains by inducing combined resistant mutations. *Applied and Environmental Microbiology, 67*, 1885–1892.

Huang, H., Lv, J., Hu, Y., Fang, Z., Zhang, K., & Bao, S. (2008). *Micromonospora rifamycinia* sp. nov., a novel actinomycete from mangrove sediments. *International Journal of Systematic and Evolutionary Microbiology, 58*(1), 17–20.

Hughes, C. C., Prieto-Davo, A., Jensen, P. R., & Fenical, W. (2008). The marinopyrroles: Antibiotics of an unprecedented structure class from a marine *Streptomyces* sp. *Organic Letters, 10*, 629–631.

Ikeda, H., Ishikawa, J., Hanamoto, A., Shinose, M., Kikuchi, H., Shiba, T., … & Ōmura, S. (2003). Complete genome sequence and comparative analysis of the industrial microorganism *Streptomyces Avermitilis*. *Nature Biotechnology, 21*, 526–531.

Imada, C., Koseki, N., Kamata, M., Kobayashi, T., & Hamada-Sato, N. (2007). Isolation and characterization of antibacterial substances produced by marine actinomycetes in the presence of seawater. *Actinomycetologica, 21*, 27–31.

Jensen, P. R., Williams, P. G., Oh, D. C., Zeigler, L., & Fenical, W. (2007). Species-specific secondary metabolite production in marine actinomycetes of the genus *Salinispora*. *Applied and Environmental Microbiology, 73*(4), 1146–1152.

Jensen, P. R., Gontang, E., Mafnas, C., Mincer, T. J., & Fenical, W. (2005). Culturable marine actinomycete diversity from tropical Pacific Ocean sediments. *Environmental Microbiology, 7*, 1039–1048.

Jose, P. A., & Jebakumar, S. R. D. (2012). Phylogenetic diversity of actinomycetes cultured from coastal multipond solar saltern in Tuticorin, India. *Aquatic Biosystems, 8*, 23.

Kalyani, A. L. T., Ramya Sravani, K. M., & Annapurna, J. (2012). Isolation and characterization of antibiotic producing actinomycetes from marine soil samples. *International Journal of Current Pharmaceutical Research, 4*(2), 109–112.

Kim, B. J., Koh, Y. H., Chun, J., Kim, C. J., Lee, S. H., Cho, M. O., … & Kook, Y. H. (2003). Differentiation of actinomycete genera based on partial *rpoB* gene sequences. *Journal of Microbiology and Biotechnology, 13*(6), 846–852.

Kimura, M. (1980). A simple method for estimating evolutionary rate of base substitutions through comparative studies of nucleotide sequences. *Journal of Molecular Evolution, 16*, 111–120.

Ko, K. S., Lee, H. K., Park, M. Y., Lee, K. H., Yun, Y. J., Woo, S. Y., Miyamoto, H., & Kook, Y. H. (2002). Application of RNA polymerase β-subunit gene (*rpoB*) sequences for the molecular differentiation of *Legionella* species. *Journal of Clinical Microbiology, 40*, 2653–2658.

Kumar, A., Saini, P., & Shrivastava, J. N. (2009). Production of peptide antifungal antibiotic and biocontrol activity of *Bacillus Subtilis*. *Indian Journal of Experimental Biology*, *47*(1), 57.

Kumar, N., Singh, R. K., Mishra, S. K., Singh, A. K., & Pachouri, U. C. (2010). Isolation and screening of soil actinomycetes as source of antibiotics active against bacteria. *International Journal of Microbiology Research, 2*(2), 12–16.

Kumar, P. S., Al-Dhabi, N. A., Duraipandiyan, V., Balachandran, C., Kumar, P. P., & Ignacimuthu, S. (2014). In vitro antimicrobial, antioxidant and cytotoxic properties of *Streptomyces lavendulae* strain SCA5. *BMC Microbiology, 14*, 291.

Lam, K. S. (2006). Discovery of novel metabolites from marine actinomycetes. *Current Opinion in Microbiology, 9*, 245–251.

Lazzarini, A., Cavaletti, L., Toppo, G., & Marinelli, F. (2000). Rare genera of actinomycetes as potential producers of new antibiotics. *Anton Leeuwenhoek, 78*, 388–405.

Lechevalier, M. P., & Lechevalier, H. (1970). Chemical composition as a criterion in the classification of aerobic actinomycetes. *International Journal of Systematic Bacteriology, 20*, 435–443.

Maleki, H., & Mashinchian, O. (2011). Characterization of *Streptomyces* isolates with UV, FTIR spectroscopy and HPLC analyses. *Bioimpacts, 1*(1), 47–52.

Manteca, A., & Sánchez, J. (2009). *Strepto myces* development in colonies and soils. *Applied and Environmental Microbiology, 75*(9), 2920–2924.

Narendhran, S., Rajiv, P., Vanathi, P., & Sivaraj, R. (2014). Spectroscopic analysis of bioactive compounds from *Streptomyces cavouresis* KUV39: Evaluation of antioxidant and cytotoxicity activity. *International Journal of Pharmacy and Pharmaceutical Sciences, 6*(7), 319–322.

Niederman, M. S. (1997). Is "crop rotation" of antibiotics the solution to a "resistant" problem in the ICU? *American Journal of Respiratory and Critical Care Medicine, 156*, 1029–1031.

Okazaki, T., & Okami, Y. (1972). Studies on marine microorganisms. II. Actinomycetes in Sagami Bay and their antibiotic substances. *Journal of Antibiotics, 25*(8), 461–466.

Oskay, A. M., Tamer, A. U., & Azeri, C. (2004). Antibacterial activity of some actinomycetes isolated from farming soil of Turkey. *African Journal of Biotechnology, 3*(9), 441–446.

Kumar, P. S., Al-Dhabi, N. A., Duraipandiyan, V., Balachandran, C., Kumar, P. P., & Ignacimuthu, S. (2014). In vitro antimicrobial, antioxidant and cytotoxic properties of *Streptomyces lavendulae* strain SCA5. *BMC Microbiology, 14*, 291.

Parungao, M. M., Maceda, E. B., & Villano, M. A. F. (2007). Screening of antibiotic-producing actinomycetes from marine, brackish and terrestrial sediments of Samal Island, Philippines. *JRSCE, 4*(3), 29–38.

Remya, M., & Vijayakumar, R. (2008). Isolation and characterization of marine antagonistic actinomycetes from west coast of India. *Medicine and Biology, 15*(1), 13–19.

Riedlinger, J., Reicke, A., Zahner, H., Krishmer, B., Bull, A. T., & Maldonado, L. A. (2004). Abyssomicins, inhibitors of the para-aminobenzoic acid pathway produced by the marine *Verrucosispora* strain AB-18-032. *Journal of Antibiotics, 57*, 271–279.

Rifaat, H. M. (2003). The biodiversity of actinomycetes in the River Nile exhibiting antifungal activity. *Journal of Mediterranean Ecology, 4*, 5–7.

Singh, L. S., Sharma, H., & Talukdar, N. C. (2014). Production of potent antimicrobial agent by actinomycete *Streptomyces sannanensis* strain SU118 isolated from phoomdi in Loktak Lake of Manipur, India. *BMC Microbiology, 14*, 278.

Suneetha, V., & Raj, K. (2011). Isolation and identification of *Streptomyces* ST1 and ST2 strains from tsunami-affected soils: Morphological and biochemical studies. *Journal of Oceanography and Marine Science, 2*(4), 96–101.

Takizawa, M., Colwell, R. R., & Hill, R. T. (1993). Isolation and diversity of actinomycetes in the Chesapeake Bay. *Applied and Environmental Microbiology, 59*(4), 997–1002.

Thenmozhi, M., & Krishnan, K. (2011). Anti-aspergillus activity of *Streptomyces* sp. VITSTK7 isolated from Bay of Bengal coast of Puducherry, India. *Journal of Natural Environmental Sciences, 2*(2), 1–8.

Valli, S., Suvathi Sugasini, S., Aysha, O. S., Nirmala, P., Vinoth Kumar, P., & Reena, A. (2012). Antimicrobial potential of actinomycetes species isolated from marine environment. *Asian Pacific Journal of Tropical Biomedicine, 9*, 416–473.

Vijayakumar, R., Muthukumar, C., Thajuddin, N., & Panneerselvam, A. (2005). Screening of antagonistic actinomycetes from the East Coast of India. In *VIII National Symposium on Soil Biology in Human Welfare* (p. 26). Ponniyah Ramajayam College, Thanjavur, Tamil Nadu, India.

Weinstein, M. P., Litvin, S. Y., & Guida, V. G. (2005). Consideration of habitat linkages, estuarine landscapes and the trophic spectrum in wetland restoration design. *Journal of Coastal Research, 40*, 51–63.

Wise, R. (2008). The worldwide threat of antimicrobial resistance. *Current Science, 95*, 181–187.

Author(s) Information

Khansa M. Younis
University of Mosul
Mosul/Iraq
Contact e-mail: *kansbio50@uomosul.edu.iq*

To cite this article:

Younis, K.M. (2025). Screening of bioactive secondary metabolites of *streptomyces spp.* Isolated from the sediments. *The Eurasia Proceedings of Health, Environment and Life Sciences (EPHELS), 20,* 32-44.

The Eurasia Proceedings of Health, Environment and Life Sciences (EPHELS)
ISSN: 2791-8033

The Eurasia Proceedings of Health, Environment and Life Sciences (EPHELS), 2025

Volume 20, Pages 45-52

ICMeHeS 2025: International Conference on Medical and Health Sciences

Unsupervised Image Segmentation

Abdelkader Khobzaoui
Djillali Liabes University of Sidi Bel Abbes

Mohammed Benhammoudda
Djillali Liabes University of Sidi Bel Abbes

Abstract: Image segmentation involves partitioning of an image into distinct regions based on criteria such as color, texture, or shape, facilitating the focused analysis of relevant objects. Among the various approaches to image segmentation, clustering algorithms, particularly K-means, have gained prominence because of their efficacy in grouping similar pixels. However, these algorithms face challenges such as predetermining the number of regions and sensitivity to initial cluster centers. These issues often result in inconsistent segmentation. This paper proposes a novel color-based segmentation approach that utilizes density function mode detection to predict suitable cluster centroids, aiming to enhance the consistency and accuracy of segmentation results. As demonstrated by various tests, the proposed method has the potential to improve the analysis in numerous domains, including object detection, facial recognition, medical imaging and remote sensing.

Keywords: Image segmentation, Clustering, K-means, Kernel density estimation (KDE), Modes

Introduction

Image segmentation is a basic technique in computer vision and image processing that involves partitioning a digital image into several segments or regions, each representing a different object or part of the image (Lei & Nandi, 2023). This process aims to simplify the representation of an image, making it easier to analyze and understand its content. In essence, image segmentation groups together pixels with similar characteristics, such as color, texture, or intensity, making it possible to identify and isolate specific objects or areas of interest in the image.

Image segmentation is the basis for many applications that we encounter on a regular basis. In healthcare, for example, it facilitates medical imaging to diagnose diseases, detect tumors, or plan surgical interventions. In autonomous vehicles, image segmentation helps to recognize pedestrians, road signs, and other vehicles, contributing to safer navigation. In smartphone cameras, it enables portrait mode by separating the subject from the background. Security systems use it for facial recognition and object detection. Even in social media, image segmentation enables functions such as augmented reality filters and automatic tagging. These different applications show the versatility of image segmentation techniques, they are classified, by Siddiqui et al. (2022), into four general categories: thresholding, clustering, edge-based segmentation technique, and region-based segmentation as shown in Figure 1.

Each of these techniques has its own strengths that make them particularly suitable for certain contexts and different performance criteria. Among these different approaches, cluster-based methods stand out due to their popularity and versatility. One of the most widely used clustering techniques in image segmentation is the K-means algorithm (MacQueen, 1967) that consists in partitioning the image pixels into a set of clusters, where each pixel is assigned to the cluster with the closest center according to the algorithm 1.

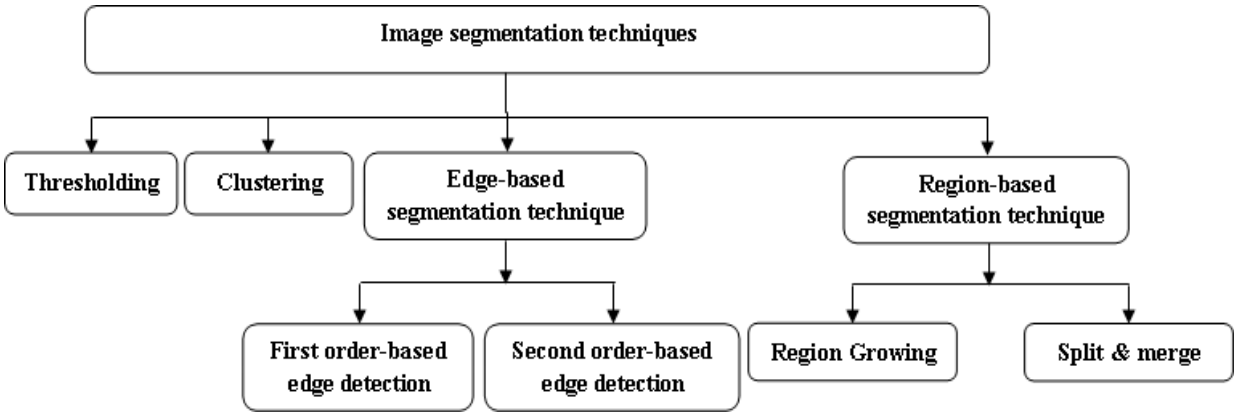

Figure 1. General classifications of the image segmentation technique(Siddiqui, 2022).

Algorithm 1. K-means Algorithm for Image Segmentation

Require:

- I : Image,
- K : number of clusters,
- *maxIter* :maximum iterations.

Ensure:

- Segmented image with K clusters

Initialize K cluster centers $\{c_1, c_2, ..., c_K\}$ randomly
$iter \leftarrow 0$
while not converged and $iter < maxIter$ **do for** each pixel p in I **do**
Assign p to nearest cluster center based on color or intensity
for $k \leftarrow 1$ to K **do**
Recalculate c_k as the mean of all pixels, p_i, in cluster k using
$iter \leftarrow iter + 1$

K-means algorithm is particularly effective for its simplicity and computational efficiency. These attributes, coupled with its ease of implementation, make it a preferred choice in many image segmentation applications, especially when combined with other prepossessing or post-processing techniques. However, the K-means algorithm also has limitations. It requires the number of clusters (K) to be specified in advance, which may not always be known. It is also sensitive to initial cluster center placement and may converge to local optima. Several variants of the K-means-based clustering algorithm have been tested to improve its performance and avoid these limitations, including integration with other techniques, improved initialization and convergence, and parallel and GPU-accelerated implementations. In this context, we propose a novel color-based segmentation approach that uses density function mode detection to predict the suitable initial cluster centroids for the K-means algorithm. After a review of related work in section 2, we introduce our novel color-based segmentation approach in section 3. We then analyze the results and discuss the implications of our findings in section 4. Finally, we conclude our study in section 5 by summarizing our findings and presenting our conclusive remarks.

Related Work

The effectiveness of the K-means algorithm in image segmentation has undergone significant enhancements through various innovations. Karbhari et al. (2018) proposed a GPU-accelerated parallel implementation of the K-means clustering algorithm for image segmentation, leveraging CUDA C on NVIDIA GPUs. This approach optimized performance by employing shared memory for efficient image data storage and constant memory for cluster data, reducing memory access latency and improving computational efficiency. This resulted in significant speedups in processing, with performance improvements ranging from 9x to 57x compared to the sequential version. Additionally, the approach scaled effectively as the number of clusters increased, further enhancing computational efficiency. Mashor(2000) introduced the moving k-means clustering algorithm, an innovative variant of the traditional k-means method that addresses several of its inherent limitations, including sensitivity to initial conditions and susceptibility to local optima.

While maintaining the core iterative process of assigning data points to the nearest centroid and updating centroids accordingly, the moving k-means algorithm introduces a key enhancement through its ”fitness” metric. This metric ensures that centroids are updated only if a cluster contains the minimum required number of data points, effectively reducing the algorithm’s vulnerability to poor initialization and local optima. As a result, the moving k-means algorithm becomes more robust to outliers and better at capturing complex data structures. These advantages make it particularly effective for segmenting microarray images, where spot sizes and intensities may vary against complex backgrounds, ensuring more accurate and reliable segmentation in challenging scenarios. The Optimized K-Means (OKM) algorithm (Siddiqui, 2012) introduced several important innovations to improve image segmentation. Unlike K-means, which assigns a pixel to the cluster with the highest variance when it is equidistant from multiple clusters, OKM assigns a pixel to a cluster with fewer members or a lower fitness value to improve cluster coherence. OKM also fixes the ”dead center” problem encountered in previous algorithms, such as moving K-means, which cannot distinguish between empty clusters and those with zero variance within clusters. By implementing these improvements, OKM avoids trapping cluster centers at local minima, a common pitfall of K-means, and thus improves the overall quality of clustering. Experimental evaluations show that OKM produces more homogeneous and accurate image segmentation, and thus represents a significant advance in K-means-based algorithms for image processing tasks.

Purohit et al. (2013) introduced another variant of K-means to enhance the initial centroid selection and the overall algorithm performance. This modified algorithm employs a systematic approach to select the initial centroids based on the Euclidean distance between the data points. By starting with the closest pairs and gradually forming sets, the algorithm improves the runtime efficiency and reduces the mean square error, demonstrating a particular efficacy with dense datasets. Additionally, Shunye (2013) proposed a novel clustering algorithm combining hierarchical clustering with k-means, leveraging a Huffman tree for initial centroid selection and the Manhattan distance for dissimilarity measurement. This method aims to improve cluster quality and stability compared with standard k-means, potentially avoiding local optima issues. Jose et al.(2014) introduced a tumor detection algorithm for MRI images that integrates k-means and fuzzy c-means clustering with machine learning classification. This hybrid approach enhances accuracy by segmenting distinct regions based on clustering, extracting features, and classifying tumor areas using classifiers, such as support vector machines or neural networks.

Adhikari et al.(2015) proposed an algorithm that combines K-means and subtractive clustering to enhance the image segmentation accuracy and efficiency. Their method integrated partial contrast stretching, initial K-means clustering, and iterative refinement using subtractive clustering, followed by thresholding for the final segmentation. Zheng et al.(2018) introduced an adaptive K-means image segmentation method based on LAB color space, enhancing segmentation robustness by adapting K-means clustering to color and texture features. Shah et al.(2021) introduce a method that integrates the Bar et al.(2011) model into the k-Means (KM) algorithm for image segmentation, addressing the limitations of standard k-Means, which often results in fragmented segments due to its focus solely on color quantization without considering pixel connectivity. The proposed Mumford–Shah k-Means (MS-KM) modifies the standard KM algorithm by incorporating a shape constraint derived from the Mumford–Shah model, optimizing both pixel similarity and segment shape using a modified distance measure. The method begins by selecting random cluster centroids and calculating image gradients. Each pixel is then assigned to a cluster based on a modified distance metric that accounts for both color similarity and boundary length, determined from the image gradient. Afterward, cluster centroids are recalculated by averaging the pixels in each segment. This process repeats until convergence, ensuring the optimization of both content similarity and segment shape. The approach effectively reduces fragmentation and produces smoother segment boundaries compared to standard k-Means while maintaining computational efficiency.

Wisaeng et al.(2022) proposed a breast cancer detection method combining K-means++ clustering with cuckoo search optimization, demonstrating superior accuracy in segmenting mammogram images into tumor and non-tumor regions. This approach enhances detection accuracy while reducing noise and improving the clarity of segmented regions. It starts with preprocessing techniques, including color normalization and noise reduction, to enhance image quality. Then, K-Means++ initializes cluster centroids for image segmentation, and CSO further optimizes these centroids by mimicking the behavior of cuckoo birds laying eggs in host nests. The segmentation process is refined using mathematical morphology and OTSU’s thresholding to highlight cancerous regions more effectively. Kalaipriya et al. (2023) presented a segmentation and classification approach for human lung cancer detection, incorporating optimization strategies. This method begins with the preprocessing of medical images, followed by a hybrid

segmentation technique that combines an enhanced k-means clustering algorithm with random forest. For classification, an artificial neural network (ANN) is employed, improved through particle swarm optimization (PSO) to optimize parameters and refine feature selection.

The proposed method in Braik et al.(2023), involves optimizing the k-means clustering algorithm using the white shark optimizer (WSO) to address the weakness of k-Means algorithm, which is its susceptibility to random initialization of the initial center. The k-Means serves as the starting point for the WSO, which then optimizes the final position. The WSO-based k-Means approach was evaluated on publicly available MRI brain tumor datasets and compared with the standard k-Means algorithm, fuzzy c-means (FCM), and other meta-heuristics. The results showed that the WSO-based k-Means outperformed the other algorithms in clustering performance. Kaur(2023) proposed an innovative hybrid image segmentation technique that integrates K-means clustering with two bio-inspired optimization methods: Particle Swarm Optimization (PSO) and the Firefly Algorithm (FA). The approach processes plant images using three comparative methods: basic K-means, K-means with PSO, and K-means with the Firefly algorithm, with the latter proving to be the most effective.

The Firefly algorithm, inspired by the flashing behavior of fireflies and their attraction mechanisms, addresses K-means' tendency to get stuck in local optima by optimizing centroid positions and discovering global solutions through improved exploration. This hybrid method achieves up to 97% segmentation accuracy and superior correlation coefficients compared to traditional methods, making it highly valuable for applications in plant disease detection, medical imaging, and content-based image retrieval. Its success lies in combining the clustering efficiency of K-means with the global optimization strengths of the Firefly algorithm, leading to more reliable and precise image segmentation in various fields. Sabha et al.(2024) focused on determining the optimal value of K for K-means clustering in color segmentation. It utilizes the Gray Level Co-occurrence Matrix (GLCM) to retrieve correlated features and calculate the aggregate probability of their occurrence based on pixel pairings. The number $\mathbf{K}$ is identified as spikes in this correlation. The results show that this approach achieves high efficiency, with an accuracy of 98%. Khan et al. (2024) proposed a nonparametric K-means clustering approach (EAIS) designed to enhance image segmentation by automatically determining the number of clusters and their initialization.

Unlike traditional clustering methods, which struggle with predefined segment numbers, EAIS adapts by utilizing five modules: deep image reconstruction for smoothing and reducing color channel variance, intra-histogram peak level detection for understanding pixel distributions, inter-histogram peak level association for linking similar clusters, mutual consensus-oriented cluster seeds merging to reduce redundancy and determine the optimal number of clusters, and morphological reconstruction-driven spatial post-processing to enhance spatial consistency within segments. The method employs image histograms to determine optimal initialization conditions and dynamically merges cluster seeds. Experimental results on the BSDS500 benchmark show that EAIS performs comparably or better than state-of-the-art methods, offering both high segmentation quality and computational efficiency.

The k-means clustering algorithm remains one of the most widely used algorithms in the literature, and many authors have compared their new proposals to k-means during validation processes. In this section, we focus exclusively on work related to image segmentation. Ahmed et al.(2020) presented a structured and comprehensive review of the k-means algorithm, discussing its limitations and the latest advances aimed at improving its capabilities and applicability within the research community. In this paper, we present a novel approach based on density function mode detection to optimize and accurately determine the initial centroids for the k-means algorithm. By overcoming the challenges associated with the selection of the initial centroids, our method aims to improve the efficiency and accuracy of the k-means clustering algorithm. This improvement leads to the identification of optimal starting points, resulting in more precise and reliable segmentation results.

Method

Our proposed image segmentation method improves the standard K-means clustering approach by integrating density function mode detection to optimize the selection of initial centroids. The procedure is outlined as follows:

1. First, the image is loaded and converted into a numerical array, where the pixel values are separated into red, green, and blue (RGB) channels. For each channel, we estimate the pixel intensity

distribution using kernel density estimation (KDE), which is given by the equation 1:

$$\hat{f}(x) = \frac{1}{nh^d} \sum_{i=1}^{n} K(\frac{x - x_0}{n}) \quad (1)$$

where n is the number of data points (pixels), d is the dimensionality (3 for the RGB color space), h is the bandwidth parameter, x_i represents the data points, and K is the kernel function. Common kernel choices include the Gaussian kernel, Epanechnikov kernel, and others. In our method, we use the Gaussian kernel, defined by equation 2 due to its smoothness properties and its ability to model data distributions effectively.

$$K(x) = \frac{1}{(2\pi)^{\frac{d}{2}}} e^{-\frac{1}{2}\|x\|^2} \quad (2)$$

Ultimately, the choice of kernel should balance smoothness and computational efficiency based on the application. Another important parameter is the bandwidth(h), which controls the width of the kernel and thus the smoothness of the estimated density function. A small bandwidth leads to a more sensitive estimation, capturing finer details but potentially overfitting the data, while a large bandwidth results in a smoother estimate that may overlook subtle variations in the data. In practice, bandwidth selection is often done via cross-validation or heuristics such as Silverman's rule of thumb, which provides an optimal bandwidth for Gaussian kernels under certain assumptions. Our method uses Silverman's rule of thumb to determine the bandwidth, balancing sensitivity and generalization to avoid overfitting or underfitting the data.

The density function obtained from KDE helps us understand the distribution of colors in the image. This step is critical for identifying areas with higher data concentration, which correspond to regions with higher pixel intensity or feature density. The kernel function smooths the data distribution, providing a continuous estimate of the underlying structure. Proper selection of both the kernel function and bandwidth is essential for accurate density estimation, which in turn allows for more reliable detection of dense areas vital for selecting suitable initial centroids in the K-means algorithm.

After estimating the density function for each color channel, we identify the prominent peaks (modes) representing significant pixel intensity levels. These 1D modes from each channel are then combined into 3D modes, forming a set of RGB color combinations representing the dominant colors in the image

The identified 3D modes serve as the initial centroids for the K-means clustering algorithm. This step ensures that the algorithm selects the optimal initial centroids in a way that avoids local maxima and ensures a better distribution of centroids across the dataset, leading to more accurate and effective clustering.

2. The algorithm groups the image pixels based on color similarity. To ensure robustness, clusters with pixel counts below a computed threshold are discarded. This threshold is calculated using the interquartile range (IQR) method, ensuring that only significant clusters contribute to the final segmentation.

3. The remaining clusters' centroids are used for the final K-means clustering step. The result is a segmented image where each pixel is assigned the color of its respective cluster centroid. The method effectively prevents the algorithm from converging to local minima by initializing centroids based on data-driven mode estimation, improving the segmentation quality.

Results and Discussion

In order to verify the efficiency and feasibility of the proposed algorithm, we tested it on the image used in Chowdhury et al.(2016), shown in Figure 2a. This benchmark image allows an initial comparison with previously published approaches and a direct visual assessment of the segmentation quality between the original image and its segmented counterpart. In our experiment, the KDE–based initialization automatically selected five significant color clusters, which were then refined by K-means. Visual inspection of Figure 2b shows that the method faithfully preserves the main structures of the scene while producing compact and homogeneous regions. Most object boundaries are sharply delineated and the background is strongly simplified,

confirming the ability of the proposed unsupervised algorithm to extract meaningful regions without any prior knowledge of the number or location of the segments

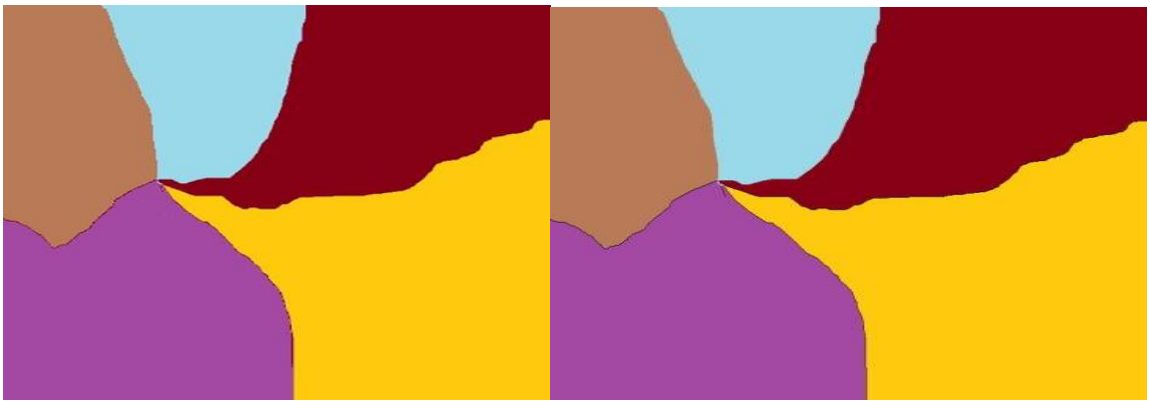

(a) Original picture (b) Segmented picture

Figure 2. Image used in the experiments

As a second experiment, we considered the synthetic ”tricolor” image composed of three partially overlapping colored disks (Figure 3a). This image is interesting because it contains a small number of well–separated colors together with mixed regions created by the overlaps and a textured background. The proposed KDE–based procedure automatically selected five significant color clusters, which K-means then refined (Figure 3b).

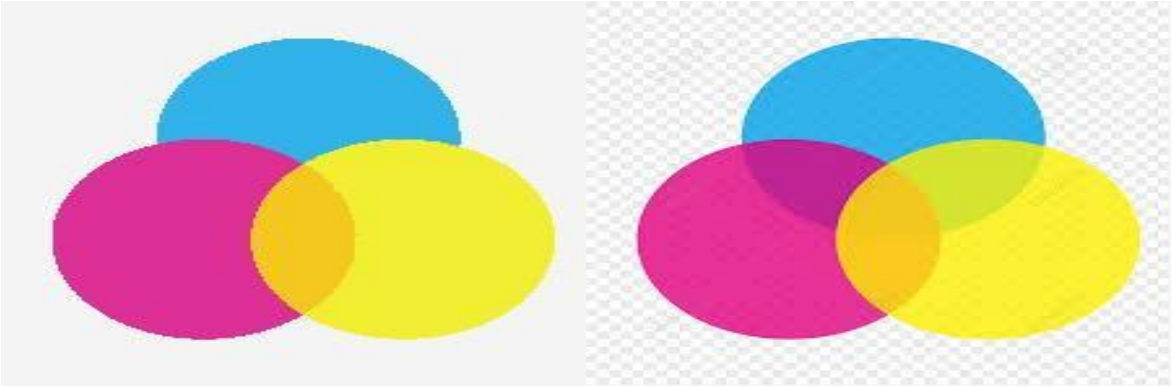

(a) Original picture (b) Segmented picture

Figure 3. Tricolor image

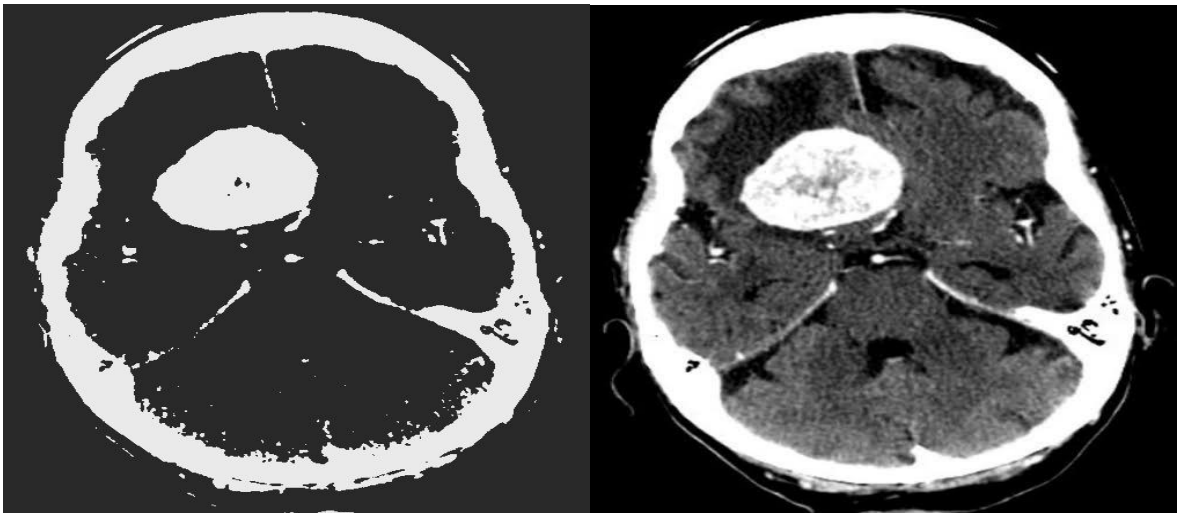

(b) Original picture (b) Segmented picture

Figure 4. Pathological brain image

The resulting segmentation clearly separates the three primary disks, the orange overlap region, and the background. In particular, the transparency grid present in the original image is almost completely removed, and the contours of the disks remain smooth and well localized, illustrating the ability of the method to recover both pure and mixed regions from multimodal color distributions. We also evaluated the proposed approach on a pathological brain slice containing a bright intra-cranial lesion (Figure 4a). The global gray-level distribution is strongly skewed, with three main modes corresponding to the dark background, the normal brain parenchyma, and very bright structures (bone and hyperdense lesion). From the estimated density functions, the KDE–based initialization retained two dominant clusters, which were then refined by K-means.

As illustrated in Figure 4b, the resulting segmentation succeeds in isolating the high-intensity structures (skull and lesion) from the rest of the brain tissue, while still providing a coherent partition of the intracranial region. This experiment suggests that the method can enhance the visual contrast between normal and abnormal regions without requiring any prior information about the lesion

Conclusion

In this work, we proposed an unsupervised color-based segmentation method that exploits kernel density estimation to detect the dominant modes of the RGB distributions and uses these modes as data-driven initial centroids for the K-means algorithm, thereby reducing the sensitivity to initialization and discarding insignificant clusters. Experiments on a natural scene, a synthetic tricolor image and pathological brain slices show that the approach preserves the main structures while producing compact and homogeneous regions, accurately separates pure and mixed color areas in multimodal distributions and yields coherent partitions on low-contrast medical images, where high-intensity abnormalities are clearly emphasized. Future research will focus on extending the framework to other color spaces and multimodal data (e.g., RGB–depth or multispectral images), integrating spatial regularization to further suppress noise and small isolated regions, conducting large-scale comparisons with state-of-the-art, including deep learning–based segmentation models, and adapting the method to interactive or semi-supervised scenarios in which limited user input can guide the segmentation process.

Scientific Ethics Declaration

* The authors declare that the scientific ethical and legal responsibility of this article published in EPHELS journal belongs to the authors.

Conflict of Interest

* The authors declare that they have no conflicts of interest

Funding

* This research received no specific grant from any funding agency in the public, commercial, or not-for-profit sectors.

Acknowledgements or Notes

* This article was presented as an oral presentation at the International Conference on Medical and Health Sciences (www.icmehes.net) held in Antalya/Türkiye on November 12-15, 2025.

References

Adhikari, S. K., Sing, J. K., Basu, D. K., & Nasipuri, M. (2015). Conditional spatial fuzzy c-means clustering algorithm for segmentation of MRI images. *Applied Soft Computing, 34*, 758–769.

Ahmed, M., Seraj, R., & Islam, S. M. S. (2020). The k-means algorithm: A comprehensive survey and performance evaluation. *Electronics, 9*(8), 1295.

Bar, L., Chan, T. F., Chung, G., Jung, M., Kiryati, N., Mohieddine, R., Sochen, N., & Vese, L. A. (2011). Mumford and Shah model and its applications to image segmentation and image restoration. In *Handbook of mathematical methods in imaging*. Springer Science & Business Media.

Braik, M., Al-Hiary, H., & Al-Betar, M. A. (2023, December). Brain tumor segmentation of MRI images based on k-means and white shark optimizer. In *2023 24th International Arab Conference on Information Technology (ACIT)* (pp. 1–8). IEEE.

Chowdhury, S., Roy, S., Mitra, A., & Das, P. (2016). Automated number of cluster determination using the combination of entropy and histogram peaks from multiple images. *International Journal of Signal Processing, Image Processing and Pattern Recognition, 9*(7), 107–116.

Jose, A., Ravi, S., & Sambath, M. (2014). Brain tumor segmentation using k-means clustering and fuzzy c-means algorithms and its area calculation. *International Journal of Innovative Research in Computer and Communication Engineering, 2*(3), 3496-3501.

Kalaipriya, O., & Dhandapani, S. (2023, December). Lung cancer detection using RF-k-means and classification with optimized ANN algorithm. *Journal of Intelligent & Fuzzy Systems*, 1–15.

Karbhari, S., & Alawneh, S. (2018, May). GPU-based parallel implementation of k-means clustering algorithm for image segmentation. In *2018 IEEE International Conference on Electro/Information Technology (EIT)* (pp. 52–57). IEEE.

Kaur, M. (2023, May). Plant disease image segmentation applying the k-means algorithm, firefly, and particle swarm optimisation. *International Journal for Research in Applied Science and Engineering Technology, 11*, 982–990.

Khan, Z., & Yang, J. (2024). Nonparametric k-means clustering-based adaptive unsupervised colour image segmentation. *Pattern Analysis and Applications, 27*(1), 17.

Lei, T., & Nandi A.K. (2023). *Image segmentation: Principles, techniques, and applications*. Wiley.

MacQueen, J. (1967). Some methods for classification and analysis of multivariate observations. In *Proceedings of the Fifth Berkeley Symposium on Mathematical Statistics and Probability* (Vol. 1, pp. 281–297). University of California Press.

Mashor, M. Y. (2000). Hybrid training algorithm for RBF network. *International Journal of the Computer, the Internet and Management, 8*(2), 50–65.

Purohit, P., & Joshi, R. (2013). A new efficient approach towards k-means clustering algorithm. *International Journal of Computer Applications, 65*(11), 7–10.

Sabha, M., & Saffarini, M. (2024). Selecting optimal k for k-means in image segmentation using GLCM. *Multimedia Tools and Applications, 83*(18), 55587–55603.

Shah, N., Patel, D., & Fränti, P. (2021). K-means image segmentation using Mumford–Shah model. *Journal of Electronic Imaging, 30*(6), 063029.

Shunye, W. (2013). An improved k-means clustering algorithm based on dissimilarity. In *Proceedings of the 2013 International Conference on Mechatronic Sciences, Electric Engineering and Computer (MEC)* (pp. 2629–2633). IEEE.

Siddiqui, F. U., & Yahya, A. (2022). *Clustering techniques for image segmentation* (1st ed.). Springer.

Siddiqui, F., & Mat Isa, N. (2012). Optimized k-means (OKM) clustering algorithm for image segmentation. *Opto-Electronics Review, 20*, 216–225.

Wisaeng, K. (2022). Breast cancer detection in mammogram images using k-means++ clustering based on cuckoo search optimization. *Diagnostics, 12*(12).

Zheng, X., Zheng, X., Lei, Q., Yao, R., Gong, Y., & Yin, Q. (2018). Image segmentation based on adaptive k-means algorithm. *EURASIP Journal on Image and Video Processing, 2018*(1), 1–13.

Author(s) Information

Abdelkader Khobzaoui
Djillali Liabes University of Sidi Bel Abbès
Algeria
Contact e-mail: *abdelkader.khobzaoui@univ-sba.dz*

Mohammed Benhammoudda
Djillali Liabes University of Sidi Bel Abbès
Algeria

To cite this article:

Khobzaoui, A., & Benhammoudda, M. 2025). Unsupervised image segmentation. *The Eurasia Proceedings of Health, Environment and Life Sciences (EPHELS), 20,* 45-52.